

Stochastic gradient descent estimation of generalized matrix factorization models with application to single-cell RNA sequencing data

Cristian Castiglione^{*1}, Alexandre Segers², Lieven Clement², and Davide Risso³

¹ *Bocconi Institute for Data Science and Analytics, Bocconi University. Via Röntgen 1, 20136 Milan, Italy*

² *Department of Applied Mathematics, Computer Science and Statistics, Ghent University. Krijgslaan 281-S9, 9000 Ghent, Belgium*

³ *Department of Statistical Sciences, University of Padova. Via Cesare Battisti 241, 35121 Padova, Italy.*

Abstract

Single-cell RNA sequencing allows the quantitation of gene expression at the individual cell level, enabling the study of cellular heterogeneity and gene expression dynamics. Dimensionality reduction is a common preprocessing step to simplify the visualization, clustering, and phenotypic characterization of samples. This step, often performed using principal component analysis or closely related methods, is challenging because of the size and complexity of the data. In this work, we present a generalized matrix factorization model assuming a general exponential dispersion family distribution and we show that many of the proposed approaches in the single-cell dimensionality reduction literature can be seen as special cases of this model. Furthermore, we propose a scalable adaptive stochastic gradient descent algorithm that allows us to estimate the model efficiently, enabling the analysis of millions of cells. Our contribution extends to introducing a novel warm start initialization method, designed to accelerate algorithm convergence and increase the precision of final estimates. Moreover, we discuss strategies for dealing with missing values and model selection. We benchmark the proposed algorithm through extensive numerical experiments against state-of-the-art methods and showcase its use in real-world biological applications. The proposed method systematically outperforms existing methods of both generalized and non-negative matrix factorization, demonstrating faster execution times while maintaining, or even enhancing, matrix reconstruction fidelity and accuracy in biological signal extraction. Finally, all the methods discussed here are implemented in an efficient open-source R package, `sgdGMF`, available at [github/CristianCastiglione/sgdGMF](https://github.com/CristianCastiglione/sgdGMF).

Keywords: Dimension reduction; Generalized linear models; Matrix factorization; Stochastic optimization; single-cell; RNA-seq.

^{*}cristian.castiglione@unibocconi.it, alexandre.segers@ugent.be, lieven.clement@ugent.be, davide.risso@unipd.it

1 Introduction

1.1 The ever-increasing single cell RNA sequencing data sets

Single-cell RNA sequencing (scRNA-seq) technologies have revolutionised the comprehension of biological processes by offering a quantitative measure of transcript abundance at the individual cell level. Single-cell resolution is critical for the study of cellular heterogeneity (Wu et al., 2023; Kim and Cho, 2023), temporal dynamics (Kouno et al., 2013; Jean-Baptiste et al., 2019), and cell-type differentiation (Denyer et al., 2019). However, the size and complexity of the data have dramatically increased compared to bulk sample-level assays, challenging statistical methods and software implementations to deal with thousands of genes profiled in millions of cells (Angerer et al., 2017; Kharchenko, 2021).

From a statistical perspective, scRNA-seq yields high-dimensional count data, in which observations (i.e., cells) lie in a $\sim 10,000$ -dimensional gene space. Working in such high-dimensional spaces poses a wealth of statistical and computational challenges. Hence, one of the first steps in the analysis of single-cell data is dimensionality reduction. Indeed, proper dimensionality reduction reduces both noise and computational complexity and simplifies downstream analyses such as data visualization, cell clustering, and lineage reconstruction (Sun et al., 2019; Kiselev et al., 2019; Xiang et al., 2021). To this end, state-of-the-art methods leverage a low-rank representation of the data to extract useful information while correcting for known confounders such as batch effects or other technical or biological covariates (Risso et al., 2018; Townes et al., 2019; Agostinis et al., 2022).

Yet, the dimensionality reduction of scRNA-seq is not trivial. This technology yields count data with low mean and large variance, leading to extremely skewed distributions with a large fraction of zeros (Hicks et al., 2018). To address zero inflation and overdispersion problems, Risso et al. (2018) introduced a zero-inflated negative binomial framework for gene-expression matrix factorization, named ZINB-WaVE. Despite its superior performance compared to other methods, ZINB-WaVE’s computational complexity renders it obsolete for the ever-increasing data volumes (Sun et al., 2019; Cao et al., 2021). Moreover, in modern UMI-based scRNA-seq datasets the need for modeling zero inflation has decreased (Townes et al., 2019; Svensson, 2020; Nguyen et al., 2023; Ahlmann-Eltze and Huber, 2023). In this regard, simpler models, such as those developed by Townes et al. (2019) and Agostinis et al. (2022), achieve similar performances with a much smaller computational burden. Nevertheless, even these methods struggle to scale with the current massive data volumes.

Consequently, biological researchers often resort to log-transformation of the scRNA-seq count tables and apply conventional principal component analysis (PCA; Ahlmann-Eltze and Huber, 2023). While this is a much faster alternative, it ignores the complex mean-variance relation and discrete nature of the data and may introduce synthetic biases due to imperfect data transformations (Townes et al., 2019). Therefore, the need for fast and memory-efficient matrix factorization tools on the original count scale still remains.

1.2 A matrix factorization perspective

The dimensionality reduction techniques mentioned above are all examples of matrix factorization, a statistical tool of fundamental importance in many theoretical and applied fields. In general, matrix factorization methods aim at decomposing the target data matrix into the product of two lower-rank matrices explaining the principal modes of variations in the observations. Such low-rank matrices are typically interpreted in terms of *factors* and *loadings*. Factors represent stochastic latent variables, i.e. random effects, lying in a small-dimensional space and determining the individual characteristics of each observation in the sample. Loadings are non-stochastic coefficients mapping the latent factors into the

observed data space, or some one-to-one transformation thereof. Specifically, in single-cell RNA-seq applications, factors and loadings can be interpreted as “meta genes” and “gene weights”, respectively (Stein-O’Brien et al., 2018). In this context, matrix factorization is usually employed to project the cells into the space of the first few factors to then cluster them in discrete groups (Kiselev et al., 2019) or infer other low-rank signal, such as pseudotime ordering (Street et al., 2018).

Principal component analysis (PCA; Jolliffe, 1986), i.e., singular value decomposition (SVD), plays a central role in the literature, being the first and most used factorization method proposed in the field. It constitutes the base for several generalizations such as probabilistic PCA (Tipping and Bishop, 1999), factor analysis, and, more generally, generalized linear latent variable models (GLLVM, Bartholomew et al., 2011). Probabilistic formulations equip PCA with a data-generating mechanism that opens the door to alternative inferential procedures, such as likelihood-based and Bayesian approaches. Moreover, it provides a natural way to simulate new synthetic signals using a proper generating mechanism induced by the likelihood specification. Assuming a Gaussian law for the data, PCA can be formulated as the solution to a likelihood maximization problem under appropriate identifiability constraints; see, e.g., Tipping and Bishop (1999). This perspective unveils why PCA may be **suboptimal** for non-Gaussian data, such as positive scores, counts, or binary observations.

Over the years, many extensions have been proposed to address the limitations of the Gaussian PCA. Some relevant examples are non-negative matrix factorization (Lee and Seung, 1999; Wang and Zhang, 2012), Binary PCA (Schein et al., 2003), Poisson PCA (Durif et al., 2019; Smallman et al., 2020; Kenney et al., 2021; Virta and Artemiou, 2023), exponential family PCA (Collins et al., 2001; Mohamed et al., 2008; Li and Tao, 2010; Gopalan et al., 2015; Wang et al., 2020), generalized linear latent variable models (Niku et al., 2017), generalized PCA (Townes et al., 2019), generalized matrix factorization (Kidziński et al., 2022) and deviance matrix factorization (Wang and Carvalho, 2023).

Non-negative matrix factorization (NMF; Lee and Seung, 1999; Wang and Zhang, 2012) decomposes positive score matrices by minimizing either the squared error loss or the Kullback-Leibler loss under non-negativity constraints for the factor and loading matrices. The exploitation of non-negative patterns proved successful in many applied fields, such as computer vision and recommendation systems, as well as omics feature extraction (Stein-O’Brien et al., 2018).

Similarly, methods based on exponential family models extend PCA by assuming a more general loss function and linking the data to the latent matrix decomposition using a smooth bijective transformation. For instance, Collins et al. (2001) considered the exponential family Bregman divergence, while Townes et al. (2019), Kidziński et al. (2022) and Wang and Carvalho (2023) considered the exponential family (negative) log-likelihood.

Exponential family generalizations of PCA, which we refer to as *generalized matrix factorization* (GMF) models, are typically estimated using alternated Fisher scoring algorithms implemented via iterative re-weighted least squares, or some modification thereof; see, e.g., Collins et al. (2001), Kidziński et al. (2022) and Wang and Carvalho (2023). Such a procedure directly extends the classical Fisher scoring algorithm for generalized linear models (McCullagh and Nelder, 1989), being a stable and easy-to-code algorithmic approach. On the other hand, in high-dimensional settings, this iterative procedure suffers two major flaws: (i) it requires multiple scans of the entire dataset during each iteration; (ii) it requires the costly numerical solution of several linear systems. It is worth noting that, for matrix factorization problems, the number of parameters to update, i.e. the number of linear systems to solve, is proportional to the dimension of the data matrix. To address points (i) and (ii) in the context of scRNA-seq, Townes et al. (2019) employed an alternated Fisher scoring method which only requires the computation of element-wise derivatives and matrix multiplications, avoiding expensive matrix inversions. In the same vein, Kidziński et al. (2022) proposed a quasi-Newton algorithm that only requires cheap

Table 1: List of the major matrix factorization models (first column) available in the literature for exponential family data. For each model, we report the corresponding R package (second column) and we describe its characteristics (from the third to the last columns). Each feature is marked with \checkmark if it is completely implemented in the package and \times otherwise. The column *Families* lists the most common distributions belonging to the exponential family along with some generalizations: Normal (N), Gamma (G), Binomial (B), Poisson (P), Negative Binomial (NB), quasi-likelihood (Q) and zero-inflated (ZI) models. The column *Effects* refers to the regression effects that can be included in the linear predictor and uses the notation introduced in Section 2, Equation (3). The column *Implementation* describes some technical features of the numerical implementation, such as the language used for the core computations (*Core*), if parallel computing is allowed (*Parallel*) and if minibatch subsample and stochastic optimization methods are available (*Stochastic*).

Package	Model	Families							Effects			Implementation		
		N	G	B	P	NB	Q	ZI	\mathbf{XB}^\top	$\mathbf{\Gamma Z}^\top$	\mathbf{UV}^\top	Core	Parallel	Stochastic
R Spectra	PCA	\checkmark	\times	\times	\times	\times	\times	\times	\times	\times	\checkmark	F/C++	\times	\checkmark
g lmpca	GMF	\times	\times	\checkmark	\checkmark	\checkmark	\times	\times	\checkmark	\checkmark	\checkmark	R	\times	\checkmark
z inbwave	GMF	\times	\times	\times	\times	\checkmark	\times	\checkmark	\checkmark	\checkmark	\checkmark	R	\checkmark	\times
n ewwave	GMF	\times	\times	\times	\times	\checkmark	\times	\times	\checkmark	\checkmark	\checkmark	R	\checkmark	\checkmark
g mf	GMF	\checkmark	\checkmark	\checkmark	\checkmark	\times	\times	\times	\checkmark	\times	\checkmark	R	\checkmark	\times
d mf	GMF	\checkmark	\checkmark	\checkmark	\checkmark	\checkmark	\checkmark	\times	\checkmark	\times	\checkmark	R	\times	\times
s gdGMF	GMF	\checkmark	\checkmark	\checkmark	\checkmark	\checkmark	\checkmark	\times	\checkmark	\checkmark	\checkmark	C++	\checkmark	\checkmark
g llvm	GLLVM	\checkmark	\checkmark	\checkmark	\checkmark	\checkmark	\times	\times	\checkmark	\checkmark	\checkmark	R	\times	\times
N MF	NMF	\checkmark	\times	\times	\checkmark	\times	\times	\times	\times	\times	\checkmark	C++	\checkmark	\times
N NLM	NMF	\checkmark	\times	\times	\checkmark	\times	\times	\times	\times	\times	\checkmark	C++	\checkmark	\times
c mfrec	NMF	\checkmark	\times	\times	\checkmark	\times	\times	\times	\checkmark	\checkmark	\checkmark	C++	\checkmark	\times

element-wise algebraic calculations. To the best of our knowledge, these are the most efficient methods proposed in the literature for the estimation of matrix factorization models under exponential family likelihood. However, in both cases, a complete pass through the data is still necessary to completely update the parameter estimates, which might be infeasible in massive data scenarios.

1.3 Our contribution

In this work, we propose a scalable stochastic optimization algorithm to tackle the complex optimization problem underlying the estimation of high-dimensional GMF models. Specifically, the proposed algorithm relies on the stochastic gradient descent (SGD) framework (Robbins and Monro, 1951; Bottou, 2010) with adaptive learning rate schedules (Duchi et al., 2011; Zeiler, 2012; Kingma and Ba, 2014; Reddi et al., 2019). By doing this, we decrease the computational complexity of the problem by using a convenient combination of minibatch subsampling, partial parameter updates and exponential gradient averaging. Additionally, we propose two efficient initialization methods, which help the convergence to a meaningful solution while reducing the likelihood of the algorithm’s convergence to highly sub-optimal stationary points.

Alongside, we propose an efficient R/C++ implementation of the proposed method in the new open-source R package **sgdGMF**, freely available on GitHub¹. Compared to alternative implementations in

¹Refer to the GitHub repository [github/CristianCastiglione/sgdGMF](https://github.com/CristianCastiglione/sgdGMF)

R, `sgdGMF` offers one of the most complete and flexible estimation frameworks for generalized matrix factorization modelling, allowing for all standard exponential family distributions, quasi-likelihood models, row- and column-specific regression effects, as well as model-based missing value imputation. Moreover, it provides several algorithms for parameter estimation, including the proposed stochastic gradient descent approach. To enhance scalability, parallel computing is employed as much as possible at any stage of the analysis, including initialization, estimation, model selection and post-processing. Table 1 compares all these features with alternative packages freely available in R.

We showcase the `sgdGMF` implementation on both simulated and real data, demonstrating the scalability of the proposed method on gene expression matrices of different dimensions. In all the numerical experiments we consider, the proposed stochastic gradient approach outperforms the alternative state-of-the-art methods in terms of execution time while having superior signal reconstruction quality, measured as out-of-sample residual deviance and cluster separation in the latent space.

The paper is organized as follows. In Section 2 we formally define the class of generalized matrix factorization models, we formulate the associated estimation problem and we discuss the connections with other models in the literature. In Section 3, we introduce the proposed stochastic optimization method building upon quasi-Newton and stochastic gradient descent algorithms; additionally, we propose an efficient approach for parameter initialization. In Section 4, we discuss different methods for model selection. In Section 5, we empirically compare the proposed algorithm with several state-of-the-art methods in the literature through an extensive simulation study. In Section 6, we propose two case studies on real datasets of medium- and high-dimensional sizes, respectively, proving the effectiveness of our approach to extract coherent biological signals while maintaining a high level of computational efficiency. Section 7 is devoted to a concluding discussion and future research directions.

2 Model specification

Let us define $\mathbf{Y} = \{y_{ij}\}$ as the $n \times m$ data matrix containing the response variables of interest, which have (i, j) th entry $y_{ij} \in \mathcal{Y} \subseteq \mathbb{R}$, i th row $\mathbf{y}_i \in \mathcal{Y}^m$ and j th column $\mathbf{y}_{:j} \in \mathcal{Y}^n$. Conventionally, y_{ij} is here considered as the i th observational unit over the j th variable, that in our genomic application are the i th cell and the j th feature/gene. Hereafter, all the vectors are column vectors and all the transposed vectors, denoted by \cdot^\top , are row vectors. To account for non-Gaussian observations, such as odds, counts, or continuous positive scores, we consider for the response variable y_{ij} an *exponential dispersion family* (EF) distribution with *natural parameter* θ_{ij} and *dispersion* ϕ , denoted by

$$y_{ij} \mid \theta_{ij} \sim \text{EF}(\theta_{ij}, \phi), \quad i = 1, \dots, n, \quad j = 1, \dots, m. \quad (1)$$

Moreover, we denote the mean and variance of y_{ij} by $\mathbb{E}(y_{ij}) = \mu_{ij}$ and $\text{Var}(y_{ij}) = a_{ij}(\phi)\nu(\mu_{ij})$, respectively. Here and elsewhere, $\nu(\cdot)$ is the family-specific variance function, which controls the heteroscedastic relationship between the mean and variance of y_{ij} , while $a_{ij}(\cdot)$ is a dispersion function specified as $a_{ij}(\phi) = \phi/w_{ij}$, with $w_{ij} > 0$ being a user-specified weight and $\phi > 0$ being a scalar dispersion parameter. Under such a model specification, the probability density function of y_{ij} can be written as

$$f(y_{ij}; \theta_{ij}, \phi) = \exp \left[\{y_{ij}\theta_{ij} - b(\theta_{ij})\} / a_{ij}(\phi) + c(y_{ij}, \phi) \right], \quad (2)$$

where $b(\cdot)$ and $c(\cdot, \cdot)$ are family-specific functions. Specifically, $b(\cdot)$ is a convex twice differentiable *cumulant function* and $c(\cdot, \cdot)$ is the so-called *log-partition function*. By the fundamental properties of the dispersion exponential family, the mean and variance of y_{ij} satisfy the identities $\mu_{ij} = \dot{b}(\theta_{ij})$ and

Table 2: Exponential family laws along with their support space, canonical link (g_c), variance (ν), and rescaled deviance ($D/2a$) functions. Here, we denote by $N \in \mathbb{N}$ and $\alpha > 0$ the size and variance parameters of the Binomial and Negative Binomial distributions, respectively.

Distribution	Support	$g_c(\mu)$	$\nu(\mu)$	$D(y, \mu)/2a(\phi)$
Gaussian	\mathbb{R}	μ	1	$(y - \mu)^2/2$
Gamma	\mathbb{R}_+	$1/\mu$	μ^2	$(y - \mu)/\mu - \log(y/\mu)$
Inv. Gauss.	\mathbb{R}_+	$1/\mu^2$	μ^3	$(y - \mu)^2/(2y\mu^2)$
Poisson	\mathbb{N}_+	$\log(\mu)$	μ	$y \log(y/\mu) - (y - \mu)$
Bernoulli	$\{0, 1\}$	$\log\{\mu/(1 - \mu)\}$	$\mu(1 - \mu)$	$y \log(y/\mu) + (1 - y) \log\{(1 - y)/(1 - \mu)\}$
Neg. Binom.	\mathbb{N}_+	$\log(\mu)$	$\mu(1 + \mu/\alpha)$	$y \log(y/\mu) - (y + \alpha) \log\{(y + \alpha)/(\mu + \alpha)\}$

$\nu(\mu_{ij}) = \ddot{b}(\theta_{ij})$, which imply $\nu(\cdot) = (\ddot{b} \circ \dot{b}^{-1})(\cdot)$, where $\dot{b}(\cdot)$ and $\ddot{b}(\cdot)$ denote the first and second derivatives of $b(\cdot)$, respectively. Therefore, $\dot{b}(\cdot)$ is a bijective map and θ_{ij} is uniquely determined by μ_{ij} .

Some relevant distributions belonging to the exponential family are, among others, the Gaussian, Inverse Gaussian, Gamma, Poisson, Binomial and Negative Binomial laws. Table 2 shows the family-specific variance functions related to these examples as well as the associated canonical link and deviance functions. We recall that the deviance function of model (2) is defined as $D(y, \mu) = -2 \log\{f_\phi(y, \mu)/f_\phi(y, y)\}$, where $f_\phi(y, \mu) = f(y; \theta, \phi)$ denotes the likelihood function relative to observation y expressed as a function of mean μ and possibly depending on dispersion ϕ .

We complete the model specification by introducing an appropriate parametrization for the conditional mean μ_{ij} . In particular, we consider the generalized multivariate regression model

$$g(\mu_{ij}) = \eta_{ij} = (\mathbf{X}\mathbf{B}^\top + \mathbf{\Gamma}\mathbf{Z}^\top + \mathbf{U}\mathbf{V}^\top)_{ij} = \mathbf{x}_{i:}^\top \boldsymbol{\beta}_{:j} + \boldsymbol{\gamma}_{i:}^\top \mathbf{z}_{:j} + \mathbf{u}_{i:}^\top \mathbf{v}_{:j}, \quad (3)$$

where $g(\cdot)$ is a continuously differentiable bijective link function and η_{ij} is a linear predictor. The latter is represented as an additive decomposition of three terms: a column-specific regression effect, $(\mathbf{X}\mathbf{B}^\top)_{ij} = \mathbf{x}_{i:}^\top \boldsymbol{\beta}_{:j}$, a row-specific regression effect, $(\mathbf{\Gamma}\mathbf{Z}^\top)_{ij} = \boldsymbol{\gamma}_{i:}^\top \mathbf{z}_{:j}$, and a residual matrix factorization $(\mathbf{U}\mathbf{V}^\top)_{ij} = \mathbf{u}_{i:}^\top \mathbf{v}_{:j}$. Specifically, $\mathbf{x}_{i:} \in \mathbb{R}^p$ and $\mathbf{z}_{:j} \in \mathbb{R}^q$ denote observed covariate vectors, $\boldsymbol{\beta}_{:j} \in \mathbb{R}^p$ and $\boldsymbol{\gamma}_{i:} \in \mathbb{R}^q$ are unknown regression coefficient vectors, while $\mathbf{u}_{i:} \in \mathbb{R}^d$ and $\mathbf{v}_{:j} \in \mathbb{R}^d$ encode latent traits explaining the residual modes of variation in the data that are not captured by the regression effects. Notice that the linear predictor can be equivalently expressed using the matrix decomposition $\eta_{ij} = (\mathbf{U}_* \mathbf{V}_*^\top)_{ij}$, where $\mathbf{U}_* = [\mathbf{X}, \mathbf{\Gamma}, \mathbf{U}]$ and $\mathbf{V}_* = [\mathbf{B}, \mathbf{Z}, \mathbf{V}]$ are partially observed low-rank matrices. In the following sections, and in particular in Section 3, we make extensive use of this more compact form hiding the star-subscript to lighten the notation and simplify the exposition. Finally, we introduce the vector of unknown parameters in the model as $\boldsymbol{\psi} = (\boldsymbol{\beta}^\top, \boldsymbol{\gamma}^\top, \mathbf{u}^\top, \mathbf{v}^\top, \phi)^\top$, where the lower-case letters represent the flat vectorization of the corresponding matrix forms; for instance, $\boldsymbol{\beta} = \text{vec}(\mathbf{B})$.

The multivariate generalized linear model in (3) is non-identifiable being invariant with respect to rotation, scaling, and sign-flip transformations of \mathbf{U} and \mathbf{V} . Then, to enforce the uniqueness of the matrix decomposition, we need to impose additional identifiability constraints. Some of the most common choices in the literature involve the following equivalent parameterizations:

- (A) **Orthonormal scores:** \mathbf{U} has orthonormal columns, $\mathbf{U}^\top \mathbf{U} = \mathbf{I}_d$, \mathbf{V} has orthogonal columns, $\mathbf{V}^\top \mathbf{V} = \boldsymbol{\Delta}^2$, the first non-zero element of each column of \mathbf{V} is positive;
- (B) **Orthonormal loadings:** \mathbf{U} has orthogonal columns, $\mathbf{U}^\top \mathbf{U} = \boldsymbol{\Delta}^2$, \mathbf{V} has orthonormal columns, $\mathbf{V}^\top \mathbf{V} = \mathbf{I}_d$, the first non-zero element of each column of \mathbf{V} is positive;

(C) **Standardizes scores:** \mathbf{U} has standardized columns, say $\mathbf{1}_n^\top \mathbf{U} / n = \mathbf{0}_d$ and $\mathbf{U}^\top \mathbf{U} / n = \mathbf{I}_d$, and \mathbf{V} is lower triangular with positive diagonal entries.

Here, $\mathbf{\Delta}^2$ denotes the diagonal matrix collecting all the non-zero singular values of $\mathbf{U}\mathbf{V}^\top$ in decreasing order, \mathbf{I}_d denotes the $d \times d$ identity matrix, $\mathbf{0}_d$ is the $d \times 1$ vector of zeros, and $\mathbf{1}_n$ is the $n \times 1$ vector of ones. Notice that any unconstrained estimate of \mathbf{U} and \mathbf{V} can be easily projected into the constrained space identified by (A), (B), or (C) by post-processing; see, e.g., Kidziński et al. (2022) and Wang and Carvalho (2023). The choice of the parametrization typically depends on the specific application and the desired interpretation of the score and loading matrices. Unless explicitly stated otherwise, we will assume that parametrization (A) is used throughout.

Following the naming convention introduced by Kidziński et al. (2022), we refer to the model specification presented so far in (1)–(3) as *generalized matrix factorization* (GMF). Alternative nomenclatures, such as *exponential family principal component analysis* (EPCA, Collins et al., 2001; Mohamed et al., 2008; Li and Tao, 2010), *generalized low-rank models* (GLRM, Udell et al., 2016), *generalized linear latent variable model* (GLLVM, Niku et al., 2017; Hui et al., 2017), *generalized principal component analysis* (glmPCA, Townes et al., 2019), *deviance matrix factorization* (DMF, Wang and Carvalho, 2023), or *generalized factor model* (GFM, Liu et al., 2023), can also be found in the literature. Straightforward extensions of the GMF specification include pseudo-likelihood models, with $f(y_{ij}; \boldsymbol{\psi}) = \exp\{-L_\phi(y_{ij}, \eta_{ij})\}$ being the negative exponential of a loss function $L_\phi(\cdot, \cdot) : \mathcal{Y} \times \mathbb{R} \rightarrow \mathbb{R}_+$. Also, vector generalized estimating equations for overdispersed data are a particular case of this more general setup.

2.1 Penalized likelihood estimation

In the statistical literature, the variables \mathbf{u}_i are called *latent factors* and, typically, are assumed to follow a standard independent d -variate Gaussian distribution. This representation provides a complete specification of the probabilistic mechanism that generated the samples \mathbf{y}_i 's, which are conditionally independent given \mathbf{u}_i 's. The marginal log-likelihood function induced by such a latent variable representation is given by

$$\sum_{i=1}^n \log \int_{\mathbb{R}^d} \left[\prod_{j=1}^m f(y_{ij} | \mathbf{u}_i) \right] f(\mathbf{u}_i) d\mathbf{u}_i, \quad (4)$$

where $f(y_{ij} | \mathbf{u}_i) = f(y_{ij}; \theta_{ij}, \phi)$ is the conditional distribution of y_{ij} given \mathbf{u}_i , while $f(\mathbf{u}_i) = \exp\{-\mathbf{u}_i^\top \mathbf{u}_i / 2\} / (2\pi)^{d/2}$ is the marginal probability density function of \mathbf{u}_i .

The unknown non-stochastic parameters can be estimated via maximum likelihood by optimizing (4). To this end, many numerical approaches have been proposed in the literature, such as Laplace approximation (Huber et al., 2004; Bianconcini and Cagnone, 2012), adaptive quadrature (Cagnone and Monari, 2013), expectation-maximization (Sammel et al., 1997; Cappé and Moulines, 2009), variational approximation (Hui et al., 2017). In practice, all these strategies perform very well in terms of accuracy but are extremely computationally expensive and do not scale well in high-dimensional problems.

An alternative approach is to treat the latent factors as if they were non-stochastic parameters and estimate them together with the other unknown coefficients. Kidziński et al. (2022) motivated this approach as a form of *penalized quasi-likelihood* (PQL, Breslow and Clayton, 1993), which is a standard tool in the estimation of *generalized linear mixed models* (GLMM, Lee et al., 2017). Formally, the PQL estimate of $\boldsymbol{\psi}$, say $\hat{\boldsymbol{\psi}}$, is the solution of

$$\hat{\boldsymbol{\psi}} = \underset{\boldsymbol{\psi} \in \Psi}{\operatorname{argmin}} \{ \ell_\lambda(\boldsymbol{\psi}; \mathbf{y}) \}, \quad (5)$$

with Ψ being the parameter space of $\boldsymbol{\psi}$, which incorporate the identifiability constrains in (A1)–(A2), and $\ell_\lambda(\boldsymbol{\psi}; \mathbf{y})$ denoting the penalized negative log-likelihood function. The latter is given by

$$\ell_\lambda(\boldsymbol{\psi}; \mathbf{y}) = - \sum_{i=1}^n \sum_{j=1}^m \log f(y_{ij}; \theta_{ij}, \phi) + \frac{\lambda}{2} \|\mathbf{U}\|_F^2 + \frac{\lambda}{2} \|\mathbf{V}\|_F^2, \quad (6)$$

where $\lambda > 0$ is a regularization parameter and $\|\cdot\|_F^2$ denotes the Frobenius norm.

In a complete data scenario, the number of observed data entries in the response matrix is nm and the total number of unknown parameters to be estimated is $pm + qn + d(n + m) + 1$. In partially observed data cases, the sum over $i \in \{1, \dots, n\}$ and $j \in \{1, \dots, m\}$ in (6), can be easily replaced with a sum over $(i, j) \in \Omega$, where $\Omega \subseteq \{1, \dots, n\} \times \{1, \dots, m\}$ is the set collecting the index-position of all the observed data in the response matrix.

The optimization problem (5) is not jointly convex in \mathbf{U} and \mathbf{V} . However, objective function (6) is bi-convex, namely it is conditional convex in \mathbf{U} given \mathbf{V} , and *vice versa*. This characteristic naturally encourages the development of iterative methods, which cycle over the alternated updates of \mathbf{U} and \mathbf{V} until convergence to a local stationary point. Similar strategies are commonly used in matrix completion and recommendation systems for the estimation of high-dimensional matrix factorization models; see, e.g., Zou et al. (2006), Koren et al. (2009) and Mazumder et al. (2010).

2.2 Related models

The GMF specified in (1)–(3) has strict connections and similarities to several models in the literature. It extends *vector generalized linear models* (VGLM, Yee, 2015), and hence also univariate generalized linear models (McCullagh and Nelder, 1989), by introducing a second regression effect, $(\boldsymbol{\Gamma}\mathbf{Z}^\top)_{ij}$, and a latent matrix factorization, $(\mathbf{U}\mathbf{V}^\top)_{ij}$, in the linear predictor, to account for additional modes of variations and residual dependence structures.

Also, GMF directly generalizes *principal component analysis* (PCA), which, by definition, is the solution of the minimization problem

$$\min_{\mathbf{u}, \mathbf{v}} \frac{1}{2} \sum_{i=1}^n \sum_{j=1}^m (y_{ij} - \mathbf{u}_i^\top \mathbf{v}_j)^2 \quad \text{subject to} \quad \mathbf{U}^\top \mathbf{U} = \mathbf{I}_d, \quad \mathbf{V}^\top \mathbf{V} = \boldsymbol{\Delta}^2.$$

Then, in the GMF notation, PCA can be obtained by assuming a Gaussian distribution for the data matrix, an identity link function for the mean and no regression effects in the linear predictor, namely $(\mathbf{X}\mathbf{B}^\top)_{ij} = 0$ and $(\boldsymbol{\Gamma}\mathbf{Z}^\top)_{ij} = 0$. Generalizations of PCA, such as Binary PCA (Schein et al., 2003; Lee et al., 2010; Landgraf, 2015; Song et al., 2019) and Poisson PCA (Kenney et al., 2021; Virta and Artemiou, 2023), are included in the GMF framework.

Close connections can also be drawn with *non-negative matrix factorization* (NMF; Wang and Zhang, 2012), which, in its more common formulations, searches for the best low-rank approximation $\mathbf{U}\mathbf{V}^\top$ of the data matrix \mathbf{Y} by minimizing either the squared error loss or the Poisson deviance under non-negativity constraints for \mathbf{U} and \mathbf{V} . Formally, the NMF solution is defined as

$$\min_{\mathbf{u}, \mathbf{v}} \sum_{i=1}^n \sum_{j=1}^m L(y_{ij}, \mathbf{u}_i^\top \mathbf{v}_j) \quad \text{subject to} \quad \mathbf{U} \geq 0, \quad \mathbf{V} \geq 0,$$

with $L(\cdot, \cdot)$ being either the squared error loss, i.e. the Gaussian deviance, or the Kullback-Leibler loss, i.e. the Poisson deviance. This representation clarifies that NMF can be written as a particular instance

of GMF for non-negative data, where Gaussian/Poisson likelihood is used together with an identity link and non-negativity constraints. Extensions of basic NMF have also been proposed to introduce external information through the inclusion of covariates; see, e.g., *collective matrix factorization* and *content-aware recommendation systems* (Singh and Gordon, 2008; Cortes, 2018).

3 Estimation algorithm

For the sake of exposition, throughout this section, we assume without loss of generality that $\mathbf{B} = \mathbf{0}$ and $\mathbf{\Gamma} = \mathbf{0}$ or, equivalently, that \mathbf{U}_* and \mathbf{V}_* are partially known matrices incorporating the regression effects and the covariate matrices. In the following, we suppress the $*$ subscript to lighten the notation. Moreover, we consider ϕ as a known fixed parameter, noting that, if unknown, it can be estimated iteration-by-iteration using either a method of moments or via maximum likelihood. More details are provided in the Appendix. Finally, we introduce the matrices $\dot{\mathbf{D}} = \{\dot{D}_{ij}\} = \{\partial\ell_\lambda/\partial\eta_{ij}\}$ and $\ddot{\mathbf{D}} = \{\ddot{D}_{ij}\} = \{\partial^2\ell_\lambda/\partial\eta_{ij}^2\}$ for the derivatives of the deviance with respect to the linear predictor, where

$$\dot{D}(y, \mu) = \frac{\partial\ell_\lambda}{\partial\eta} = \frac{w(y - \mu)}{\phi\nu(\mu)\dot{g}(\mu)}, \quad \ddot{D}(y, \mu) = \frac{\partial^2\ell_\lambda}{\partial\eta^2} = \frac{w\alpha(\mu)}{\phi\nu(\mu)\{\dot{g}(\mu)\}^2},$$

and $\alpha(\mu) = 1 + (y - \mu)\{\dot{\nu}(\mu)/\nu(\mu) + \ddot{g}(\mu)/\dot{g}(\mu)\}$. Accordingly, we define $\dot{g} = dg/d\mu$, $\ddot{g} = d^2g/d\mu^2$ and $\dot{\nu} = d\nu/d\mu$. Notice that the expected second-order derivative, i.e., the Fisher weight $\mathbb{E}(\ddot{D}_{ij})$, just corresponds to the observed second-order differential \ddot{D}_{ij} with $\alpha(\mu_{ij}) = 1$, which is positive for any y_{ij} and μ_{ij} .

The penalized estimate $\hat{\psi}$ in (5), say the vectorized concatenation of $\hat{\mathbf{U}}$ and $\hat{\mathbf{V}}$, must satisfy the first-order matrix conditions

$$\frac{\partial\ell_\lambda}{\partial\mathbf{U}} = \dot{\mathbf{D}}\mathbf{V} + \lambda\mathbf{U} = 0, \quad \frac{\partial\ell_\lambda}{\partial\mathbf{V}} = \dot{\mathbf{D}}^\top\mathbf{U} + \lambda\mathbf{V} = 0, \quad (7)$$

where the differentiation is performed element-wise. Using the same formulation, we may also express the second-order derivatives of (6) as

$$\frac{\partial^2\ell_\lambda}{\partial\mathbf{U}^2} = \ddot{\mathbf{D}}(\mathbf{V} * \mathbf{V}) + \mathbf{\Lambda} > 0, \quad \frac{\partial^2\ell_\lambda}{\partial\mathbf{V}^2} = \ddot{\mathbf{D}}^\top(\mathbf{U} * \mathbf{U}) + \mathbf{\Lambda} > 0, \quad (8)$$

where $*$ is the Hadamard product and $\mathbf{\Lambda}$ is a matrix of appropriate dimensions filled by λ .

Conditionally on \mathbf{V} , the left matrix equation in (7) can be decomposed into n multivariate equations row-by-row, $\partial\ell_\lambda/\partial\mathbf{u}_i = 0$ ($i = 1, \dots, n$), that can be solved independently in parallel. The existence and uniqueness of the solution of each row-equation are guaranteed under mild regularity conditions on the exponential family and the link function. In the same way, the right matrix equation in (7) can be split into m independent vector equations, $\partial\ell_\lambda/\partial\mathbf{v}_j = 0$ ($j = 1, \dots, m$), to be solved in parallel. See, e.g., Kidziński et al. (2022) and Wang and Carvalho (2023) for a detailed discussion and derivation on (7) and (8). Notice that, in case of partially known matrices, say \mathbf{U}_* and \mathbf{V}_* , the derivatives in (7) must be replaced by $\partial\ell_\lambda/\partial[\mathbf{A}, \mathbf{U}]$ and $\partial\ell_\lambda/\partial[\mathbf{B}, \mathbf{V}]$ to exclude from the differentiation the covariate matrices \mathbf{X} and \mathbf{Z} .

3.1 Fisher scoring and quasi-Newton algorithms

The first, and most popular, algorithm introduced in the literature for finding the solution of (7) is the *alternated iterative re-weighted least squares* (AIRWLS, Collins et al., 2001; Li and Tao, 2010; Risso et al.,

2018; Kidziński et al., 2022; Wang and Carvalho, 2023; Liu et al., 2023) method. It cycles between the conditional updates of \mathbf{U} and \mathbf{V} solving the equations in (7) in a row-wise manner, using standard Fisher scoring for GLMs (McCullagh and Nelder, 1989). The resulting routine is statistically motivated, easy to implement and allows for efficient parallel computing.

However, in massive data settings, it becomes infeasible when the dimension of the problem increases in the sample size or the latent space rank. One iteration of the algorithm, i.e., a complete update of \mathbf{U} and \mathbf{V} , needs $O((n+m)d^3 + nmd)$ floating point operations to be performed, where the leading term proportional to d^3 comes from a matrix inversion that must be computed at least $n+m$ times per iteration. This is particularly limiting in real-data applications, since d is unknown *a priori* and must be selected in a data driven way, which might require fitting the model several times and for an increasing number of d , which scales cubically.

To overcome this issue, Kidziński et al. (2022) proposed a quasi-Newton algorithm which employs an approximate inversion only using the diagonal elements of the Fisher information matrix. With this simplification, only elementary matrix operations are performed reducing the computational complexity to $O((n+m)d + nmd)$. In formulas, the quasi-Newton algorithm of Kidziński et al. (2022) updates the parameter estimates at iteration t as

$$\boldsymbol{\psi}^{t+1} \leftarrow \boldsymbol{\psi}^t + \rho_t \boldsymbol{\Delta}_{\boldsymbol{\psi}}^t, \quad \boldsymbol{\Delta}_{\boldsymbol{\psi}}^t = -(\mathbf{G}_{\boldsymbol{\psi}}^t / \mathbf{H}_{\boldsymbol{\psi}}^t), \quad (9)$$

where $\{\rho_t\}$ is a sequence of learning rate parameters, $\boldsymbol{\Delta}_{\boldsymbol{\psi}}^t$ is the search direction, while $\mathbf{G}_{\boldsymbol{\psi}}^t = \partial \ell_{\lambda}^t / \partial \boldsymbol{\psi}$ and $\mathbf{H}_{\boldsymbol{\psi}}^t = \partial^2 \ell_{\lambda}^t / \partial \boldsymbol{\psi}^2$ denote respectively the first two derivatives of $\ell_{\lambda}(\boldsymbol{\psi}; \mathbf{y})$ with respect to $\boldsymbol{\psi}$ evaluated at $\boldsymbol{\psi}^t$. Throughout, \leftarrow stands for the assignment operator and the division is performed element-wise.

Exploiting the block structure of $\boldsymbol{\psi}$, the joint update (9) can be written in the coordinate-wise form

$$\begin{aligned} \mathbf{U}^{t+1} &\leftarrow \mathbf{U}^t + \rho_t \boldsymbol{\Delta}_{\mathbf{U}}^t, & \boldsymbol{\Delta}_{\mathbf{U}}^t &= -(\mathbf{G}_{\mathbf{U}}^t / \mathbf{H}_{\mathbf{U}}^t), \\ \mathbf{V}^{t+1} &\leftarrow \mathbf{V}^t + \rho_t \boldsymbol{\Delta}_{\mathbf{V}}^t, & \boldsymbol{\Delta}_{\mathbf{V}}^t &= -(\mathbf{G}_{\mathbf{V}}^t / \mathbf{H}_{\mathbf{V}}^t). \end{aligned} \quad (10)$$

where $\mathbf{G}_{\mathbf{U}}$, $\mathbf{G}_{\mathbf{V}}$, $\mathbf{H}_{\mathbf{U}}$ and $\mathbf{H}_{\mathbf{V}}$ can be obtained as in (7) and (8). Algorithm 1 provides a step-by-step pseudo-code description of the quasi-Newton method of Kidziński et al. (2022). To the best of our knowledge, this is the most efficient algorithm in the literature for the estimation of GMF models.

In what follows, we build upon the quasi-Newton algorithm of Kidziński et al. (2022) to derive an efficient stochastic optimization method that, for our purposes, should further improve the scalability of GMF modelling in high-dimensional settings.

3.2 Stochastic gradient descent

Stochastic gradient descent (SGD, Bottou, 2010) provides an easy and effective strategy to handle complex optimization problems in massive data applications. Similarly to deterministic gradient-based methods, SGD is an iterative optimization procedure which updates the parameter vector $\boldsymbol{\psi}$ until convergence following the approximate steepest descent direction, say $\hat{\boldsymbol{\Delta}}_{\boldsymbol{\psi}}^t = -\hat{\mathbf{G}}_{\boldsymbol{\psi}}^t$. Here, the hat-notation, $\hat{\mathbf{G}}_{\boldsymbol{\psi}}^t$, stands for an unbiased stochastic estimate of $\mathbf{G}_{\boldsymbol{\psi}}^t$. Under mild regularity conditions on the optimization problem and the learning rate sequence, specifically $\sum_{t=0}^{\infty} \rho_t = \infty$ and $\sum_{t=0}^{\infty} \rho_t^2 < \infty$, SGD is guaranteed to converge to a stationary point of the objective function (Robbins and Monro, 1951). A standard choice for the learning rate sequence is $\rho_t = k_0 / (1 + k_0 k_1 t)^{\tau}$ for $k_0, k_1 > 0$ and $\tau \in (1/2, 1]$, where k_0 is the initial stepsize, k_1 is a decay rate parameter, and τ determines the asymptotic tail behaviour of the sequence for $t \rightarrow \infty$.

Algorithm 1: Pseudo-code description of the quasi-Newton algorithm of Kidziński et al. (2022).
On the right, we report the computation complexity of each step.

Initialize $\mathbf{U}, \mathbf{V}, \boldsymbol{\eta}, \boldsymbol{\mu}, \phi$;

while *convergence is not reached* **do**

 Compute the likelihood derivatives

$$\boldsymbol{\eta}^t \leftarrow \mathbf{U}^t \mathbf{V}^{t\top}; \quad \boldsymbol{\mu}^t \leftarrow g^{-1}(\boldsymbol{\eta}^t); \quad O(nmd)$$

$$\dot{\mathbf{D}}^t \leftarrow \mathbf{W} * (\mathbf{Y} - \boldsymbol{\mu}^t) / \{\phi^t \nu(\boldsymbol{\mu}^t) * \dot{g}(\boldsymbol{\mu}^t)\}; \quad O(nm)$$

$$\ddot{\mathbf{D}}^t \leftarrow \mathbf{W} / \{\phi^t \nu(\boldsymbol{\mu}^t) * \dot{g}(\boldsymbol{\mu}^t)^2\}; \quad O(nm)$$

 Compute the batch gradients and update \mathbf{V}

$$\mathbf{G}_V^t \leftarrow \dot{\mathbf{D}}^{t\top} \mathbf{U}^t - \lambda \mathbf{V}^t; \quad \mathbf{H}_V^t \leftarrow \ddot{\mathbf{D}}^{t\top} (\mathbf{U}^t * \mathbf{U}^t) - \boldsymbol{\Lambda}; \quad O(nmd)$$

$$\boldsymbol{\Delta}_V^t \leftarrow -(\mathbf{G}_V^t / \mathbf{H}_V^t); \quad \mathbf{V}^{t+1} \leftarrow \mathbf{V}^t + \rho_t \boldsymbol{\Delta}_V^t; \quad O(md)$$

 Compute the batch gradients and update \mathbf{U}

$$\mathbf{G}_U^t \leftarrow \dot{\mathbf{D}}^t \mathbf{V}^t - \lambda \mathbf{U}^t; \quad \mathbf{H}_U^t \leftarrow \ddot{\mathbf{D}}^t (\mathbf{V}^t * \mathbf{V}^t) - \boldsymbol{\Lambda}; \quad O(nmd)$$

$$\boldsymbol{\Delta}_U^t \leftarrow -(\mathbf{G}_U^t / \mathbf{H}_U^t); \quad \mathbf{U}^{t+1} \leftarrow \mathbf{U}^t + \rho_t \boldsymbol{\Delta}_U^t; \quad O(nd)$$

Orthogonalize $\hat{\mathbf{U}}$ and $\hat{\mathbf{V}}$;

3.2.1 Improving naïve stochastic gradient

In the past two decades, an active area of research built upon naïve SGD to improve its convergence speed, robustify the search path against erratic perturbations in the gradient estimate and introduce locally adaptive learning rate schedules using approximate second-order information. Some examples are Nesterov acceleration (Nesterov, 1983), SGD-QN (Bordes et al., 2009), AdaGrad (Duchi et al., 2011), AdaDelta (Zeiler, 2012), RMSProp (Hinton et al., 2012), Adam (Kingma and Ba, 2014), AMSGrad (Reddi et al., 2019). Inspired by this line of literature, we propose the following *adaptive stochastic gradient descent* (aSGD) updating rule

$$\boldsymbol{\psi}^{t+1} \leftarrow \boldsymbol{\psi}^t + \rho_t \boldsymbol{\Delta}_\psi^t, \quad \boldsymbol{\Delta}_\psi^t = -\alpha_t (\bar{\mathbf{G}}_\psi^t / \bar{\mathbf{H}}_\psi^t), \quad (11)$$

where $\bar{\mathbf{G}}_\psi^t$ and $\bar{\mathbf{H}}_\psi^t$ are smoothed estimates of the derivatives of (6), while α_t is a scalar bias-correction factor. Similarly to Adam (Kingma and Ba, 2014) and AMSGrad (Reddi et al., 2019), we update the smoothed gradients, $\bar{\mathbf{G}}_\psi^t$ and $\bar{\mathbf{H}}_\psi^t$, using an exponential moving average of the previous gradient values and the current stochastic estimates $\hat{\mathbf{G}}_\psi^t$ and $\hat{\mathbf{H}}_\psi^t$, namely

$$\bar{\mathbf{G}}_\psi^t \leftarrow (1 - \alpha_1) \bar{\mathbf{G}}_\psi^{t-1} + \alpha_1 \hat{\mathbf{G}}_\psi^t, \quad \bar{\mathbf{H}}_\psi^t \leftarrow (1 - \alpha_2) \bar{\mathbf{H}}_\psi^{t-1} + \alpha_2 \hat{\mathbf{H}}_\psi^t, \quad (12)$$

with $\alpha_1, \alpha_2 \in (0, 1]$ being user-specified smoothing coefficients; $\alpha_t = (1 - \alpha_2^t) / (1 - \alpha_1^t)$ is introduced to filter out the bias induced by the exponential moving average in (12). Similar smoothing techniques have two main advantages: they speed up the convergence using the inertia accumulated by previous gradients and, at the same time, they stabilize the optimization reducing the noise around the gradient estimate. We refer the reader to Kingma and Ba (2014) and Reddi et al. (2019) for a deeper discussion on the benefits of bias corrected exponential gradient averaging in high-dimensional stochastic optimization problems.

Differently from the original implementation of Adam (Kingma and Ba, 2014), which only involves first-order information, we scale the smoothed gradient estimate using a smoothed diagonal Hessian

approximation. This strategy allows us to directly extend the diagonal quasi-Newton algorithm of Kidziński et al. (2022) in a stochastic vein without increasing the computational overload or the stability of the optimization. Indeed, the derivatives of the deviance function of a GLM model are always well-defined, bounded away from zero, available in closed form and easy to compute. This is not the case for deep neural networks and other machine learning models for which Adam and AMSGrad have been originally developed.

Similarly to representation (10) for GMF models, also (11) can be written in the block-wise form

$$\begin{aligned}\mathbf{U}^{t+1} &\leftarrow \mathbf{U}^t + \rho_t \boldsymbol{\Delta}_U^t, & \boldsymbol{\Delta}_U^t &= -\alpha_t(\bar{\mathbf{G}}_U^t/\bar{\mathbf{H}}_U^t), \\ \mathbf{V}^{t+1} &\leftarrow \mathbf{V}^t + \rho_t \boldsymbol{\Delta}_V^t, & \boldsymbol{\Delta}_V^t &= -\alpha_t(\bar{\mathbf{G}}_V^t/\bar{\mathbf{H}}_V^t).\end{aligned}\tag{13}$$

In this formulation, update (10) and (13) have a computational complexity proportional to the dimension of the matrices \mathbf{U} and \mathbf{V} , namely $O((n+m)d)$. Since the dimension of the parameter space can not be further compressed without losing prediction power, the alternative way to speed up the computations is to find an efficient way for approximating the gradients, $\hat{\mathbf{G}}_\psi^t = (\hat{\mathbf{G}}_U^t, \hat{\mathbf{G}}_V^t)$ and $\hat{\mathbf{H}}_\psi^t = (\hat{\mathbf{H}}_U^t, \hat{\mathbf{H}}_V^t)$.

Exploiting the additive structure of the penalized log-likelihood in (6), a natural unbiased estimate of its derivatives can be obtained via sub-sampling. In particular, we can estimate the log-likelihood gradient by summing up only a small fraction of the data contributions, which we refer to as a *minibatch*, instead of the whole dataset. This strategy is highly scalable and can be calibrated on the available computational resources.

In what follows, we discuss a new stochastic optimization method for GMF models based on formula (13), which use local parameter updates along with minibatch estimates of the current gradients to reduce the computational complexity of the resulting algorithm. To this end, we introduce the following notation: $I = \{i_1, \dots, i_{n_I^*}\} \subseteq \{1, \dots, n\}$ is a subset of row-indices of dimension n_I^* , $J = \{j_1, \dots, j_{m_J^*}\} \subseteq \{1, \dots, m\}$ is a subset of column-indices of dimension m_J^* , $B = I \times J$ is the Cartesian product between I and J . Finally, $\mathbf{Y}_{I:} = \{\mathbf{y}_{i:}\}_{i \in I}$, $\mathbf{Y}_{:J} = \{\mathbf{y}_{:j}\}_{j \in J}$ and $\mathbf{Y}_B = \{y_{ij}\}_{(i,j) \in B}$ denote the corresponding sub-matrices, also called *row-*, *column-* and *block-minibatch* subsamples of the original data matrix, respectively.

3.2.2 Block-wise adaptive stochastic gradient descent

Both the exact and stochastic quasi-Newton methods identified by equations (10) and (13) entirely update \mathbf{U} and \mathbf{V} at each iteration. Despite being an effective and parallelizable strategy, in many applicative contexts, when it comes to factorizing huge matrices, an entire update of the parameters could be extremely expensive in terms of memory allocation and execution time. This is a well-understood issue in the literature on recommendation systems, where standard matrix completion problems may involve matrices with millions of rows and columns; see, e.g., Koren et al. (2009), Mairal et al. (2010), Recht and Ré (2013), Mensch et al. (2017). Moreover, batch optimization strategies do not generalize well to stream data contexts, where the data arrive sequentially and the parameters have to be updated on-the-fly as a new set of observations comes in.

A classic solution is to perform iterative element-wise SGD steps using only one entry of the data matrix, y_{ij} , at each iteration, thus updating the low-rank decomposition matrices row-by-row through the paired equations $\mathbf{u}_{i:}^{t+1} \leftarrow \mathbf{u}_{i:}^t - \rho_t \mathbf{G}_{U,i:}^t$ and $\mathbf{v}_{j:}^{t+1} \leftarrow \mathbf{v}_{j:}^t - \rho_t \mathbf{G}_{V,j:}^t$. In the matrix factorization literature, this strategy is also known as *online* SGD algorithm, since it permits to update the parameter estimates dynamically when a new observation is gathered.

To stabilize the optimization and speed up the convergence, we generalize the online SGD approach in two directions: we consider local stochastic quasi-Newton updates in place of naïve gradient steps and

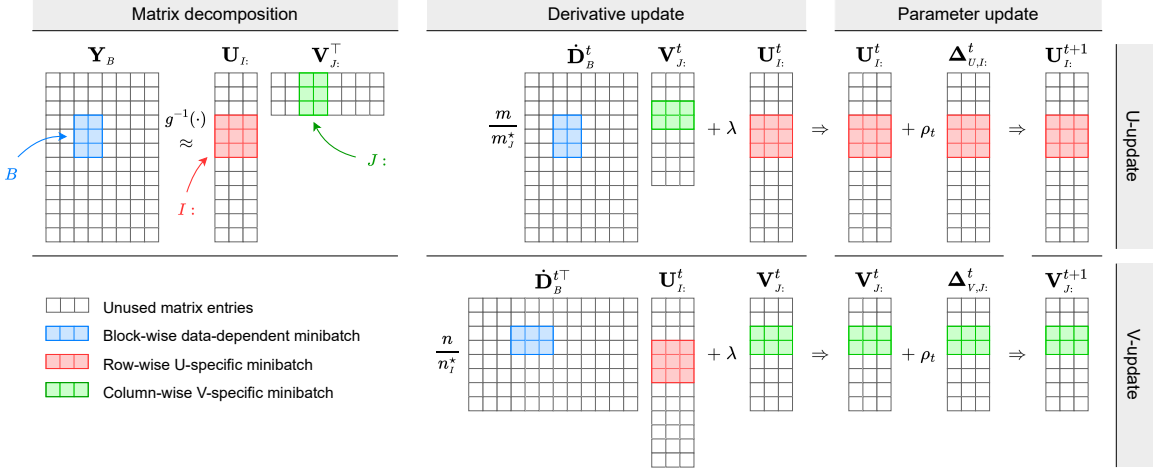


Figure 1: Graphical representation of the stochastic gradient updates employed at the t th iteration of Algorithm 2. First column: generalized matrix factorization model. Second column: matrix operations employed to obtain the gradients of the penalized log-likelihood. Third column: adaptive gradient step for updating the parameters. The coloured cells highlight the sub-sampled data used for the t th update. Empty cells represent the data not used at the t th update. To save space, the calculations of the second-order differentials and the gradient smoothing are not displayed here.

we use block-wise minibatches of the original data matrix, \mathbf{Y}_B , instead of singletons, y_{ij} . In formulas, the algorithm we propose cycles over the following adaptive gradient steps:

$$\begin{aligned} \mathbf{U}_{I,:}^{t+1} &\leftarrow \mathbf{U}_{I,:}^t + \rho_t \Delta_{U,I,:}^t, & \Delta_{U,I,:}^t &= -\alpha_t (\bar{\mathbf{G}}_{U,I,:}^t / \bar{\mathbf{H}}_{U,I,:}^t), \\ \mathbf{V}_{J,:}^{t+1} &\leftarrow \mathbf{V}_{J,:}^t + \rho_t \Delta_{V,J,:}^t, & \Delta_{V,J,:}^t &= -\alpha_t (\bar{\mathbf{G}}_{V,J,:}^t / \bar{\mathbf{H}}_{V,J,:}^t). \end{aligned} \quad (14)$$

The smoothed gradients are then estimated by exponential average as in (12) and the minibatch stochastic gradients are obtained as

$$\begin{aligned} \hat{\mathbf{G}}_{U,I,:}^t &= (m/m_J^*) \dot{\mathbf{D}}_B^t \mathbf{V}_{J,:}^t + \lambda \mathbf{U}_{I,:}^t, & \hat{\mathbf{H}}_{U,I,:}^t &= (m/m_J^*) \ddot{\mathbf{D}}_B^t (\mathbf{V}_{J,:}^t * \mathbf{V}_{J,:}^t) + \mathbf{\Lambda}, \\ \hat{\mathbf{G}}_{V,J,:}^t &= (n/n_I^*) \dot{\mathbf{D}}_B^{t\top} \mathbf{U}_{I,:}^t + \lambda \mathbf{V}_{J,:}^t, & \hat{\mathbf{H}}_{V,J,:}^t &= (n/n_I^*) \ddot{\mathbf{D}}_B^{t\top} (\mathbf{U}_{I,:}^t * \mathbf{U}_{I,:}^t) + \mathbf{\Lambda}. \end{aligned} \quad (15)$$

Here, $(m/m_J^*) (\dot{\mathbf{D}}_B^t \mathbf{V}_{J,:}^t)_{ih} = (m/m_J^*) \sum_{j \in J} \dot{D}_{ij}^t v_{jh}^t$ is an unbiased stochastic estimate of $(\dot{\mathbf{D}}^t \mathbf{V})_{ih} = \sum_{j=1}^m \dot{D}_{ij}^t v_{jh}^t$ for $i \in I$. Similarly, it is easy to show that the other minibatch averages in (15) are unbiased estimates of the corresponding batch quantities. Algorithm 2 provides a pseudo-code description of the proposed procedure, while Figure 1 provides a graphical representation of the updates.

If the dispersion parameter ϕ is unknown and has to be estimated from the data, we can also adopt a smoothed stochastic estimator obtained through exponential averaging. More details are provided in the Appendix.

We refer to (14) as *local* or *partial* updates since they just modify the rows of \mathbf{U} and \mathbf{V} corresponding to the minibatch block of indices $B = I \times J$. On the opposite, we refer to updates (10) and (13) as *global* updating rules.

Algorithm 2: Pseudo-code description of the block-wise adaptive SGD algorithm described in Section 3.2.2. On the right, we report the computational complexity of each step.

Initialize $\mathbf{U}, \mathbf{V}, \boldsymbol{\eta}, \boldsymbol{\mu}, \phi$;
Sample a random partition $\{I_1, \dots, I_R\}$ such that $\cup_{r=1}^R I_r = \{1, \dots, n\}$;
Sample a random partition $\{J_1, \dots, J_S\}$ such that $\cup_{s=1}^S J_s = \{1, \dots, m\}$;
while *convergence is not reached* **do**
 for $J \in \{J_1, \dots, J_S\}$ **do**
 Sample the minibatch set
 Sample $I \in \{I_1, \dots, I_R\}$ and set $B \leftarrow I \times J$; $O(1)$
 Compute the subsampled likelihood derivatives
 $\hat{\boldsymbol{\eta}}_B^t \leftarrow \mathbf{U}_I^t \mathbf{V}_J^{t\top}; \quad \boldsymbol{\mu}_B^t \leftarrow g^{-1}(\hat{\boldsymbol{\eta}}_B^t);$ $O(n_I^* m_J^* d)$
 $\hat{\mathbf{D}}_B^t \leftarrow \mathbf{W}_B * (\mathbf{Y}_B - \boldsymbol{\mu}_B^t) / \{\phi^t \nu(\boldsymbol{\mu}_B^t) * \dot{g}(\boldsymbol{\mu}_B^t)\};$ $O(n_I^* m_J^*)$
 $\hat{\mathbf{D}}_B^t \leftarrow \mathbf{W}_B / \{\phi^t \nu(\boldsymbol{\mu}_B^t) * \dot{g}(\boldsymbol{\mu}_B^t)^2\};$ $O(n_I^* m_J^*)$
 Compute the smoothed gradients and update \mathbf{V}
 $\hat{\mathbf{G}}_{V,J}^t \leftarrow (n/n_I^*) \hat{\mathbf{D}}_B^{t\top} \mathbf{U}_I^t - \lambda \mathbf{V}_J^t; \quad \hat{\mathbf{H}}_{V,J}^t \leftarrow (n/n_I^*) \hat{\mathbf{D}}_B^{t\top} (\mathbf{U}_I^t * \mathbf{U}_I^t) - \boldsymbol{\Lambda};$ $O(n_I^* m_J^* d)$
 $\bar{\mathbf{G}}_{V,J}^t \leftarrow (1 - \alpha_1) \bar{\mathbf{G}}_{V,J}^{t-1} + \alpha_1 \hat{\mathbf{G}}_{V,J}^t; \quad \bar{\mathbf{H}}_{V,J}^t \leftarrow (1 - \alpha_2) \bar{\mathbf{H}}_{V,J}^{t-1} + \alpha_2 \hat{\mathbf{H}}_{V,J}^t;$ $O(m_J^* d)$
 $\Delta_{V,J}^t \leftarrow -\alpha_t (\bar{\mathbf{G}}_{V,J}^t / \bar{\mathbf{H}}_{V,J}^t); \quad \mathbf{V}_J^{t+1} \leftarrow \mathbf{V}_J^t + \rho_t \Delta_{V,J}^t;$ $O(m_J^* d)$
 Compute the smoothed gradients and update \mathbf{U}
 $\hat{\mathbf{G}}_{U,I}^t \leftarrow (m/m_J^*) \hat{\mathbf{D}}_B^t \mathbf{V}_J^t - \lambda \mathbf{U}_I^t; \quad \hat{\mathbf{H}}_{U,I}^t \leftarrow (m/m_J^*) \hat{\mathbf{D}}_B^t (\mathbf{V}_J^t * \mathbf{V}_J^t) - \boldsymbol{\Lambda};$ $O(n_I^* m_J^* d)$
 $\bar{\mathbf{G}}_{U,I}^t \leftarrow (1 - \alpha_1) \bar{\mathbf{G}}_{U,I}^{t-1} + \alpha_1 \hat{\mathbf{G}}_{U,I}^t; \quad \bar{\mathbf{H}}_{U,I}^t \leftarrow (1 - \alpha_2) \bar{\mathbf{H}}_{U,I}^{t-1} + \alpha_2 \hat{\mathbf{H}}_{U,I}^t;$ $O(n_I^* d)$
 $\Delta_{U,I}^t \leftarrow -\alpha_t (\bar{\mathbf{G}}_{U,I}^t / \bar{\mathbf{H}}_{U,I}^t); \quad \mathbf{U}_I^{t+1} \leftarrow \mathbf{U}_I^t + \rho_t \Delta_{U,I}^t;$ $O(n_I^* d)$
 Orthogonalize $\hat{\mathbf{U}}$ and $\hat{\mathbf{V}}$;

The choice between alternated least squares (Kidziński et al., 2022; Wang and Carvalho, 2023), exact quasi-Newton (Algorithm 1; Kidziński et al., 2022) and the proposed block-wise stochastic gradient descent (Algorithm 2, Figure 1) methods is up to the researcher and, in principle, depends on the dimension of the problem under study and on the available computational resources. In general, algorithms using a higher amount of information are more stable, reliable and accurate; however, they tend to scale poorly in high-dimensional settings. On the other hand, cheaper methods that use less information scale well in big-data problems at the cost of a lower level of precision.

3.3 Missing value imputation

Whenever the input data matrix is only partially complete and we need to maximize (6) over the set of observed data, it is necessary to properly handle the missing values during the estimation process. To this end, we rely on the general framework proposed by Cai et al. (2010) and Mazumder et al. (2010), and later used by Kidziński et al. (2022). Intuitively, it prescribes imputing the missing data entries during the optimization by updating them at each iteration using the most recent prediction of those values.

To formally describe this imputation scheme, we define $P_\Omega(\mathbf{Y})$ as the projection of \mathbf{Y} onto its observed entries, say $P_\Omega(\mathbf{Y})_{ij} = y_{ij}$ if $(i, j) \in \Omega$ and 0 elsewhere. Similarly, we define $P_\Omega^\perp(\mathbf{Y})$ as the complementary projection of $P_\Omega(\mathbf{Y})$, such that $\mathbf{Y} = P_\Omega(\mathbf{Y}) + P_\Omega^\perp(\mathbf{Y})$. Then, in missing value situations, Algorithm 1

and 2 can be adapted by replacing the static (incomplete) data matrix \mathbf{Y} with its completed version \mathbf{Y}^t obtained at iteration t . And, at the end of each iteration, we introduce the imputation step as

$$\mathbf{Y}^{t+1} \leftarrow P_{\Omega}(\mathbf{Y}) + P_{\Omega}^{\perp}(\boldsymbol{\mu}^{t+1}).$$

As discussed by Mazumder et al. (2010), under the squared-error loss, this online imputation strategy corresponds to an expectation-maximization algorithm, where the missing values are treated as latent variables to be estimated along all the other parameters in a coordinate-wise fashion. In our case, where general exponential family likelihoods are considered and no explicit solutions are available, we can interpret the online estimation of the missing values as an approximated version of the expectation-maximization algorithm.

3.4 Parameter initialization

As is common for non-convex optimization problems, the performance of Algorithm 2 is strongly influenced by the initial values used to start the optimization cycle. Random initialization may increase the likelihood of convergence to sub-optimal local minima or unstable saddle points. Also, the convergence speed of the algorithm strongly depends on the initial parameter choice. For these reasons, it is fundamental to design good initialization strategies to improve the behaviour of the algorithm and the quality of the final estimates. Here, we propose a deterministic initialization procedure which is compliant with the model assumptions and provide a good approximation of the model at the optimum.

We leverage the conditional GLM structure of model (3) to estimate the regression parameters, $\beta_{j\cdot}$'s and $\gamma_{i\cdot}$'s, solving a sequence of independent likelihood maximization problems. We denote the resulting initial values as $\tilde{\beta}_{j\cdot}$'s and $\tilde{\gamma}_{i\cdot}$'s. Specifically, at the first stage, we estimate the column-specific regression parameters, $\beta_{j\cdot}$'s, fitting m GLMs via standard numerical solvers, e.g., Fisher scoring. Next, we follow the same strategy to estimate the row-specific regression parameters, $\gamma_{i\cdot}$'s, conditionally on the estimated column-specific effects, $\mathbf{x}_{i\cdot}^{\top} \tilde{\beta}_{j\cdot}$, which are used as offset terms. To extract the initial latent score matrix, \mathbf{U} , we follow the null-residual strategy proposed by Townes et al. (2019), which consists of computing the first d left eigenvectors of a properly defined residual matrix of the model. Common specifications for such a matrix follow the standard definition of either deviance or Pearson residuals, respectively $r_{ij}^D = \text{sign}(y_{ij} - \mu_{ij}) \sqrt{D(y_{ij}, \mu_{ij})}$ and $r_{ij}^P = (y_{ij} - \mu_{ij}) / \sqrt{\nu(\mu_{ij})}$. Here, the conditional mean of y_{ij} can be approximated using the regression effects estimated at the first two stages of the initialization, say $\tilde{\mu}_{ij} = g^{-1}(\mathbf{x}_{i\cdot}^{\top} \tilde{\beta}_{j\cdot} + \tilde{\gamma}_{i\cdot}^{\top} \mathbf{z}_{j\cdot})$. Finally, we compute the initial loading matrix, \mathbf{V} , fitting m column-specific GLMs using the matrix of latent scores $\tilde{\mathbf{U}}$ as it was a fixed design matrix and including an offset term in the linear predictor to account for both row- and column-specific regression effects, say $\mathbf{x}_{i\cdot}^{\top} \tilde{\beta}_{j\cdot} + \tilde{\gamma}_{i\cdot}^{\top} \mathbf{z}_{j\cdot}$.

Algorithm 3 provides a pseudo-code description of the proposed initialization procedure, henceforth referred to as GLM-SVD. Using standard numerical solvers to obtain the GLM solutions and the incomplete singular value decomposition, the overall computational complexity of the initialization is of order

$$m \underbrace{O(p^3 + p^2n)}_{\beta\text{-inner cycle}} + n \underbrace{O(q^3 + q^2m)}_{\gamma\text{-inner cycle}} + \underbrace{O((p+q+d)nm)}_{\mathbf{U}\text{-residual svd}} + m \underbrace{O(d^3 + d^2n)}_{\mathbf{V}\text{-inner cycle}}.$$

It is worth noticing that each step of the procedure involving GLM fitting is highly parallelizable, where each independent subroutine has at most a computational complexity of $O(k^3 + k^2n)$ where $k = \max(p, q, d)$. Improved rates can be obtained by employing alternative solvers, such as coordinate ascent (Friedman et al., 2007, 2010) or stochastic gradient methods (Toulis and Airolidi, 2015; Tran et al., 2015).

Algorithm 3: Pseudo-code description of the GLM–SVD initialization algorithm described in Section 3.4. On the right, we report the computation complexity of each step. The compact notation `glm.fit()` and `svd()` follow the naming conventions used in the corresponding R functions, assuming that a suitable model family, say EF, has been selected.

Memory allocation

$$\tilde{\boldsymbol{\eta}} \leftarrow \mathbf{0}_{n \times m}; \quad \tilde{\mathbf{B}} \leftarrow \mathbf{0}_{m \times p}; \quad \tilde{\boldsymbol{\Gamma}} \leftarrow \mathbf{0}_{n \times q};$$

Initialization of \mathbf{B}

$$\begin{array}{l} \text{for } j = 1, \dots, m \text{ do} \\ \left[\begin{array}{l} \tilde{\boldsymbol{\beta}}_{:j} \leftarrow \text{glm.fit}(\mathbf{x} = \mathbf{X}, \mathbf{y} = \mathbf{y}_{:j}, \text{offset} = \tilde{\boldsymbol{\eta}}_{:j}, \text{family} = \text{EF}); \\ \tilde{\boldsymbol{\eta}}_{:j} \leftarrow \tilde{\boldsymbol{\eta}}_{:j} + \mathbf{X}\tilde{\boldsymbol{\beta}}_{:j}; \end{array} \right. \end{array} \quad \begin{array}{l} O(p^3 + p^2n) \\ O(pn + n) \end{array}$$

Initialization of $\boldsymbol{\Gamma}$

$$\begin{array}{l} \text{for } i = 1, \dots, n \text{ do} \\ \left[\begin{array}{l} \tilde{\boldsymbol{\gamma}}_{i:} \leftarrow \text{glm.fit}(\mathbf{x} = \mathbf{Z}, \mathbf{y} = \mathbf{y}_{i:}, \text{offset} = \tilde{\boldsymbol{\eta}}_{i:}, \text{family} = \text{EF}); \\ \tilde{\boldsymbol{\eta}}_{i:} \leftarrow \tilde{\boldsymbol{\eta}}_{i:} + \mathbf{Z}\tilde{\boldsymbol{\gamma}}_{i:}; \end{array} \right. \end{array} \quad \begin{array}{l} O(q^3 + q^2m) \\ O(qm + m) \end{array}$$

Initialization of \mathbf{U}

$$\tilde{\boldsymbol{\mu}} \leftarrow g^{-1}(\tilde{\boldsymbol{\eta}}); \quad \tilde{\mathbf{R}} \leftarrow \text{resid}(\mathbf{Y}, \tilde{\boldsymbol{\mu}}); \quad \tilde{\mathbf{U}}, \tilde{\mathbf{D}}, \tilde{\mathbf{V}} \leftarrow \text{svd}(\tilde{\mathbf{R}}); \quad O(dnm + nm)$$

Initialization of \mathbf{V}

$$\begin{array}{l} \text{for } j = 1, \dots, m \text{ do} \\ \left[\begin{array}{l} \tilde{\mathbf{v}}_{:j} \leftarrow \text{glm.fit}(\mathbf{x} = \tilde{\mathbf{U}}, \mathbf{y} = \mathbf{y}_{:j}, \text{offset} = \tilde{\boldsymbol{\eta}}_{:j}, \text{family} = \text{EF}); \\ \tilde{\boldsymbol{\eta}}_{:j} \leftarrow \tilde{\boldsymbol{\eta}}_{:j} + \tilde{\mathbf{U}}\tilde{\mathbf{v}}_{:j}; \end{array} \right. \end{array} \quad \begin{array}{l} O(d^3 + d^2n) \\ O(dn + n) \end{array}$$

As an alternative strategy for high-dimensional settings, we propose to approximate the GLM estimates using a misspecified Gaussian model over a link-based transformation of the response matrix, say $y_{\varepsilon,ij} = g_{\varepsilon}(y_{ij})$. We adopt the perturbed link function $g_{\varepsilon}(\cdot)$ in place of $g(\cdot)$ to prevent the occurrence of infinite values when evaluating the link transformation, a common adjustment for binary and count data. Then, we can initialize the regression coefficient and the loading matrices solving sequentially the following least squares problems: $\min_{\boldsymbol{\beta}} \|\mathbf{Y}_{\varepsilon} - \mathbf{X}\mathbf{B}^{\top}\|^2$, $\min_{\boldsymbol{\gamma}} \|\mathbf{Y}_{\varepsilon} - \mathbf{X}\tilde{\mathbf{B}}^{\top} - \boldsymbol{\Gamma}\mathbf{Z}^{\top}\|^2$ and $\min_{\mathbf{U}, \mathbf{V}} \|\mathbf{Y}_{\varepsilon} - \mathbf{X}\tilde{\mathbf{B}}^{\top} - \boldsymbol{\Gamma}\mathbf{Z}^{\top} - \tilde{\mathbf{U}}\mathbf{V}^{\top}\|^2$. We can compute the factor scores $\tilde{\mathbf{U}}$ using the same residual decomposition discussed so far. Algorithm 4 provides a pseudo-code description of this second initialization procedure, which reduces the computation complexity of the initialization to

$$\underbrace{O(p^3 + p^2n + pnm)}_{\beta\text{-least squares}} + \underbrace{O(q^3 + q^2m + qnm)}_{\gamma\text{-least squares}} + \underbrace{O((p + q + d)nm)}_{\mathbf{U}\text{-residual SVD}} + \underbrace{O(d^3 + d^2n + dnm)}_{\mathbf{V}\text{-least squares}}.$$

By doing so, the cubic and quadratic terms in p , q and d are no longer multiplied by an external factor dependent on n or m . As a consequence, the overall computation complexity is $O\{(p^3 + q^3 + d^3) + (p^2n + q^2m + d^2n) + (p + q + d)nm\}$. Hence, in high-dimensional settings with $\max(p, q, d) \ll \min(n, m)$, the computational cost is dominated by the leading term $(p + q + d)nm$. We refer to such an approximation as OLS–SVD.

While inspired by the null-residual strategy of Townes et al. (2019), our proposed initialization methods diverge from their approach in four key aspects. Firstly, our method is exclusively employed as an initialization strategy and is not utilized as an approximation to the final estimates. Secondly,

Algorithm 4: Pseudo-code description of the OLS-SVD initialization algorithm described in Section 3.4. On the right, we report the computation complexity of each step.

Data transformation	$\mathbf{Y}_\varepsilon \leftarrow g_\varepsilon(\mathbf{Y}); \quad \tilde{\boldsymbol{\eta}} \leftarrow \mathbf{0}_{n \times m};$	$O(nm)$
Initialization of \mathbf{B}	$\tilde{\mathbf{B}} \leftarrow (\mathbf{Y}_\varepsilon - \tilde{\boldsymbol{\eta}})^\top \mathbf{X} (\mathbf{X}^\top \mathbf{X})^{-1}; \quad \tilde{\boldsymbol{\eta}} \leftarrow \tilde{\boldsymbol{\eta}} + \mathbf{X} \tilde{\mathbf{B}}^\top;$	$O(p^3 + p^2n + pnm)$
Initialization of Γ	$\tilde{\Gamma} \leftarrow (\mathbf{Y}_\varepsilon - \tilde{\boldsymbol{\eta}}) \mathbf{Z} (\mathbf{Z}^\top \mathbf{Z})^{-1}; \quad \tilde{\boldsymbol{\eta}} \leftarrow \tilde{\boldsymbol{\eta}} + \tilde{\mathbf{A}} \mathbf{Z}^\top;$	$O(q^3 + q^2n + qnm)$
Initialization of \mathbf{U}	$\tilde{\boldsymbol{\mu}} \leftarrow g^{-1}(\tilde{\boldsymbol{\eta}}); \quad \tilde{\mathbf{R}} \leftarrow \text{resid}(\mathbf{Y}, \tilde{\boldsymbol{\mu}}); \quad \tilde{\mathbf{U}}, \tilde{\mathbf{D}}, \tilde{\mathbf{V}} \leftarrow \text{svd}(\tilde{\mathbf{R}});$	$O(dnm + nm)$
Initialization of \mathbf{V}	$\tilde{\mathbf{V}} \leftarrow (\mathbf{Y}_\varepsilon - \tilde{\boldsymbol{\eta}})^\top \tilde{\mathbf{U}} (\tilde{\mathbf{U}}^\top \tilde{\mathbf{U}})^{-1};$	$O(d^3 + d^2n + dnm)$

our proposal is adaptable to any exponential family model, unlike the original approximation, which was tailored solely for count observations and lacked direct applicability to binary or continuous data. Thirdly, our proposal explicitly addresses covariate-dependent sampling schemes; in contrast, the original implementation by Townes and co-authors relied on an independent approximation of the null-residuals based on the properties of the contingency table representation of the response matrix. Lastly, our regression-based strategy for computing the loading matrix ensures that the solution approximately satisfies a proper conditional estimating equation, whereas the left eigenvectors employed in the null-residual approach do not guarantee the nullification of a proper score equation.

4 Model selection

In the GMF formulation detailed in Section 2, the model complexity is mainly controlled by the rank of the matrix factorization, d . Rank selection in matrix factorization problems is a complex research problem far from being solved. As for many other methods in statistics, the optimal selection of the factorization rank needs a careful balance between model complexity and goodness of fit to avoid both under- and over-fitting issues. In the matrix factorization literature, four main approaches can be adopted for the rank selection.

Eigenvalue thresholding criteria. The first method is to rely on the so-called *eigenvalue thresholding*, or *elbow*, criterion. It involves analyzing the singular values, in descending order, of a sufficiently high-rank matrix decomposition. The point at which we can detect a significant decrease in the rate of change of the singular values suggests the optimal number of factors to retain. This point signifies the balance between capturing sufficient variance in the data and avoiding overfitting. Thanks to its simplicity, computational efficiency, and the significant amount of empirical and theoretical support, eigenvalue thresholding methods gained wide popularity for conventional rank selection problems. See, e.g., the work of Onatski (2010), Fan et al. (2022) and Wang and Carvalho (2023). Such a class of selection criteria favors a compact low-rank representation of the signal and is often used when it is of interest to identify the principal modes of variation in the data for interpretation purposes.

Information-based criteria. The second approach is to select the unknown rank by minimizing some appropriate information criteria, such as the Akaike (AIC) or the Bayesian (BIC) information. The *information*, in these cases, is defined as an adaptation measure which tries to balance an in-sample goodness-of-fit summary, the negative log-likelihood function, and a complexity score which typically depends on the sample size and on the number of unknown parameters to be estimated. For instance, in the proposed GMF model, the sample size corresponds to the number of available entries in the data matrix, nm for complete data, and the dimension of the parameter space is $nq + mp + (n + m)d + 1$. Such a model selection criterion can be quite expensive since it requires the estimation of several models, one for each rank to be tested. However, computations can be accelerated by considering clever warm start strategies within a forward/backward stagewise estimation approach. Unfortunately, there are no guarantees that different information criteria give similar solutions, at least for finite samples.

Out-of-sample error criteria. The third rank determination method proposed in the literature leverages the concept of *out-of-sample* error minimization. An estimate of the out-of-sample error for matrix factorization problems can be obtained by holding out a bunch of entries of the data matrix during the estimation and then looking at the reconstruction error either after or even during the optimization process. The same strategy can be performed repeatedly within a cross-validation procedure to obtain a more reliable estimate of the generalization error. Then, having an error measure for a grid of ranks, we can pick the value minimizing the error. Such an approach is very popular in the machine-learning community for evaluating the performances of recommendation systems, collaborative filtering and matrix completion models, where the main goal is to obtain an accurate reconstruction of the unobserved entries of the response matrix; see, e.g., Koren et al. (2009) and Owen and Perry (2009) for an extensive statistically flavoured discussion. Rank selection based on error minimization is intuitive, general and fairly robust with respect to the optimization method used for the estimation. However, it might become extremely expensive in terms of computational resources and is highly sensitive to the selection method used for choosing the hold-out set.

Implicit selection via regularization. An additional mechanism to control model complexity in the GMF framework is to tune the regularization parameter λ in (6), which controls the amount of shrinkage enforced over the latent matrices \mathbf{U} and \mathbf{V} . Frobenius regularization is often introduced for numerical stability issues, but it is also intrinsically connected to the rank determination problem. Indeed, for any $\lambda > 0$, the Frobenius norm penalty implicitly shrinks the singular values of the matrix factorization toward zero encouraging compact low-rank representations of the signal. This spectral penalization effect and its connection with the nuclear norm has been extensively discussed in, e.g., Witten et al. (2009), Mazumder et al. (2010) and Kidziński et al. (2022). In particular, Kidziński et al. (2022) proposed to implicitly select the optimal number of latent factors in GMF problems by estimating an over-parametrized factorization with fixed rank $d \propto \sqrt{m}$ over a fine grid of λ -values and minimizing some appropriate error criterion over λ . The estimation can be efficiently performed using a pathwise optimization scheme with warm start initialization (Friedman et al., 2007). Still, it requires the estimation of several over-parametrized GMF models on a fine grid of regularization parameters, which could be quite expensive.

Generally, there is a lack of consensus in the literature regarding the optimal rank selection method, with the choice often contingent upon the objective of the analysis. In exploratory studies aimed at visually uncovering latent structures and interpreting them, eigenvalue-based methods are commonly employed, favouring more conservative approximations. Conversely, for prediction or reconstruction tasks, methods relying on information criteria and out-of-sample error are typically preferred.

In our study, we focus on single-cell RNA sequencing, in which matrix factorization plays a crucial role as a preprocessing tool to remove noise and reduce the dimensionality of the problem. Subsequently, downstream analysis steps, typically in the form of clustering or pseudotime inference, are employed to glean insightful biological information from the latent score and loading matrices. In this context, we advocate for eigenvalue-based rank selection methods, akin to those explored by Wang and Carvalho (2023). Nevertheless, the computational advantages offered by our stochastic optimization approach could also substantially benefit prediction scenarios, particularly when multiple high-dimensional models need to be fitted to minimize appropriate error criteria across a fine grid of tuning parameters.

5 Simulation studies

In this section, we assess the relative performances of the proposed estimation algorithms compared to state-of-the-art methods through several simulation experiments. In particular, we are interested in evaluating the considered approaches in terms of execution time, out-of-sample prediction error, and biological signal extraction quality.

In real data scenarios, the functional form of the data-generating mechanism is typically unknown to the researcher, and the assumption of correct model specification is rarely met. To mimic this realistic situation, in our experiments, we used different models for data simulation and signal extraction. In this way, all the estimation methods we consider are misspecified by construction and, a priori, none of them has an advantage over the others.

5.1 Data generating process

To simulate the data, we use the R package `splatter` (Zappia et al., 2017), which is freely available on Bioconductor (Huber et al., 2015). The package `splatter` allows us to simulate gene-expression matrices incorporating several user-specified features, such as the dimension of the matrix, the number of cell-types, the proportion of each cell-type in the sample, the form of the cell-type clusters, the expression level, the number of batches, the strength of the batch effects, and many others.

In our experiments, we considered the following simulation setting: each dataset contains cells from five well-separated types evenly distributed in the sample. The data are also divided into three batches having different expression levels. No lineage or branching effects are considered.

To evaluate the performance of the proposed method under different regimes, we consider two simulation settings. In simulation setting A, we compare several matrix factorization models and algorithms under a fixed latent space rank, $d = 5$, and we let the dimensions of the response matrix increase. Specifically, we set the number of cells, n , to be 10 times the number of genes, m , and we set $m \in \{100, 250, 500, 750, 1000\}$. In simulation setting B, we compare the same set of factorization methods by fixing the dimensions of the response matrix to $n = 5000$ and $m = 500$, and letting the latent space rank grow, i.e., $d \in \{5, 10, 15, 20, 25\}$. For each combination of latent rank, d , number of cells, n , and number of genes, m , under the two scenarios, we generated 100 expression matrices.

Additional details are provided in the supplementary material. Moreover, the code to generate the data and run the simulations is publically available on GitHub².

²Refer to the GitHub repository [github/alexandresegers/sgdGMF_Paper](https://github.com/alexandresegers/sgdGMF_Paper)

5.2 Competing methods and performance measures

For the estimation, we consider several matrix factorization methods based on different model specifications coming from the statistical, machine learning, or bioinformatics literature. In the following, we list all the methods we consider for signal extraction of the latent variables:

- CMF: collective matrix factorization with non-negativity constraints and batch indicator as side information matrix (`cmfrec` package; Cortes, 2023);
- NMF: non-negative matrix factorization based on the Poisson deviance without side information matrix and automatic missing value estimation mechanism (`NMF` package; Gaujoux and Seoighe, 2010);
- NMF+: non-negative matrix factorization based on the Poisson deviance without side information matrix, where the missing values are automatically estimated together with the latent variables (`NNLM` package; Lin and Boutros, 2020);
- AvaGrad: Poisson GMF model estimated using the AvaGrad algorithm (`glmPCA` package; Townes et al., 2019);
- Fisher: Poisson GMF model estimated via alternated diagonal Fisher scoring (`glmPCA` package; Townes et al., 2019);
- NBWaVE: Negative Binomial GMF estimated via alternated Fisher scoring (`NewWave` package; Agostinis et al., 2022);
- AIRWLS: Poisson GMF model estimated using the alternated iterative re-weighted least squares algorithm of Kidziński et al. (2022) and Wang and Carvalho (2023) (`sgdGMF` package; this work);
- Newton: Poisson GMF model estimated using the exact quasi-Newton algorithm of Kidziński et al. (2022) described in Algorithm 1 (`sgdGMF` package; this work);
- SGD: Poisson GMF model estimated using the proposed adaptive stochastic gradient descent with block-wise subsampling described in Algorithm 2 (`sgdGMF` package; this work)

Some of the most relevant characterizing features of all these methods and the relative implementations are summarized in Table 1. To emulate a conventional usage of all these packages, we tried to adhere closely to the standard option setups recommended in the documentation provided by their respective authors. All the algorithms implemented in the `sgdGMF` package are initialized with Algorithm 4. For more details, we refer to the Appendix. Additionally, for all methods allowing parallel computing, we run the estimation employing 4 cores. Notice that such a configuration is commonly supported by modern PCs.

To assess the relative performance of the models under consideration, we train them on a designated *training* set and subsequently evaluate their goodness-of-fit using a *validation* set. In each simulation scenario, we initially generate a complete data matrix and then construct the training set by introducing a predetermined percentage of missing values, typically set at 30%. The positions of such holdout entries are sampled from a uniform distribution on the matrix indices. The corresponding test set comprises all observations withheld during the training phase. We evaluate the models in terms of elapsed execution time (in seconds), out-of-sample reconstruction, and cell-type separation in the estimated latent space. Let \mathcal{T} and \mathcal{V} be the index sets corresponding to the training and validation entries of the response matrix and let $\bar{y}_{\mathcal{T}}$ be the empirical average of the training matrix. The out-of-sample reconstruction error is then computed using the relative Poisson deviance, that is

$$\text{Deviance}(\mathbf{Y}, \hat{\boldsymbol{\mu}}) = \sum_{(i,j) \in \mathcal{V}} D(y_{ij}, \hat{\mu}_{ij}) \bigg/ \sum_{(i,j) \in \mathcal{V}} D(y_{ij}, \bar{y}_{\mathcal{T}}).$$

To assess the degree of cell-type cluster separation over the estimated latent space, we compute two validation scores: the average silhouette width (Rousseeuw, 1987) computed on a two-dimensional t-SNE embedding (Van der Maaten and Hinton, 2008), and the neighborhood purity (Manning et al., 2008) evaluated on the original latent space.

5.3 Simulation results

Fig. 2 presents an overview of the results obtained from the data simulated with $n = 5000$, $m = 500$, and $d = 5$. Panel A shows that the proposed SGD method is the fastest implementation, while performing similarly to the best performing methods in terms of out-of-sample error and silhouette width. Panel B shows, on an exemplar simulation run, that all the GMF methods are able to reconstruct the original cell-type clustering, with the exception of AvaGrad, which is unable to separate the different groups. On the other hand the NMF methods over-cluster the data, unable to remove the simulated batch effects. This is confirmed by the average silhouette width (bottom plot of panel A) that shows a large difference in the performance of NMF and GMF methods.

These results are confirmed across both setting A and B (Fig. 3): in terms of computational efficiency, the proposed SGD implementation consistently outperforms its competitors across both settings, showing lower elapsed execution times and a better scalability with respect to both the sample size and the dimension of the latent space (Fig. 3A). Among the alternative methods, Newton emerges as the fastest, while NBWaVE and AIRWLS exhibit similar performances, which is unsurprising given their shared algorithmic strategies. On the other hand, Fisher and AvaGrad optimizers display inferior scalability compared to SGD, Newton, AIRWLS and NBWaVE (Fig. 3A). Contrary to the claims in the `glmPCA` package documentation, our findings indicate that the AvaGrad optimizer often lacks in both speed and reliability when compared to the Fisher optimizer, which typically achieves convergence within a reasonable time and, on average, runs faster than AvaGrad.

Regarding non-negative matrix factorization, implementations such as NMF and CMF demonstrate poor computational scalability across both settings. However, NMF+ shows improved performance, reaching efficiency levels close to NBWaVE and AIRWLS (Fig. 3A).

In terms of goodness-of-fit, a notable distinction arises between non-negative and generalized matrix factorization methods. Typically, GMF-based approaches consistently yield lower values of relative residual deviance compared to their NMF-based counterparts (top row of Fig. 3B). However, two exceptions to this trend are evident with NMF+ performing well and AvaGrad performing poorly. Among all compared methods, SGD consistently emerges as the most accurate approach in terms of residual deviance (top row of Fig. 3B).

The difference in performance between NMF and GMF methods becomes even clearer when looking at the silhouette width and neighborhood purity scores (middle and bottom rows of Fig. 3B). In both scenarios A and B, NBWaVE, AIRWLS, and Newton consistently outperform CMF, NMF, and NMF+. While SGD exhibits slightly suboptimal performance compared to NBWaVE, AIRWLS, and Newton, especially in small sample settings, it converges towards them as the sample size increases. This behaviour is not unexpected, as stochastic optimization algorithms typically require a large number of observations to mitigate their intrinsic randomness, achieving stability as the data dimension grows.

6 Real data applications

In this section, we will demonstrate the effectiveness of our method using two real datasets. The first dataset, referred to as the Arigoni dataset, is a 10X Genomics scRNA-seq experiment on lung cancer cell

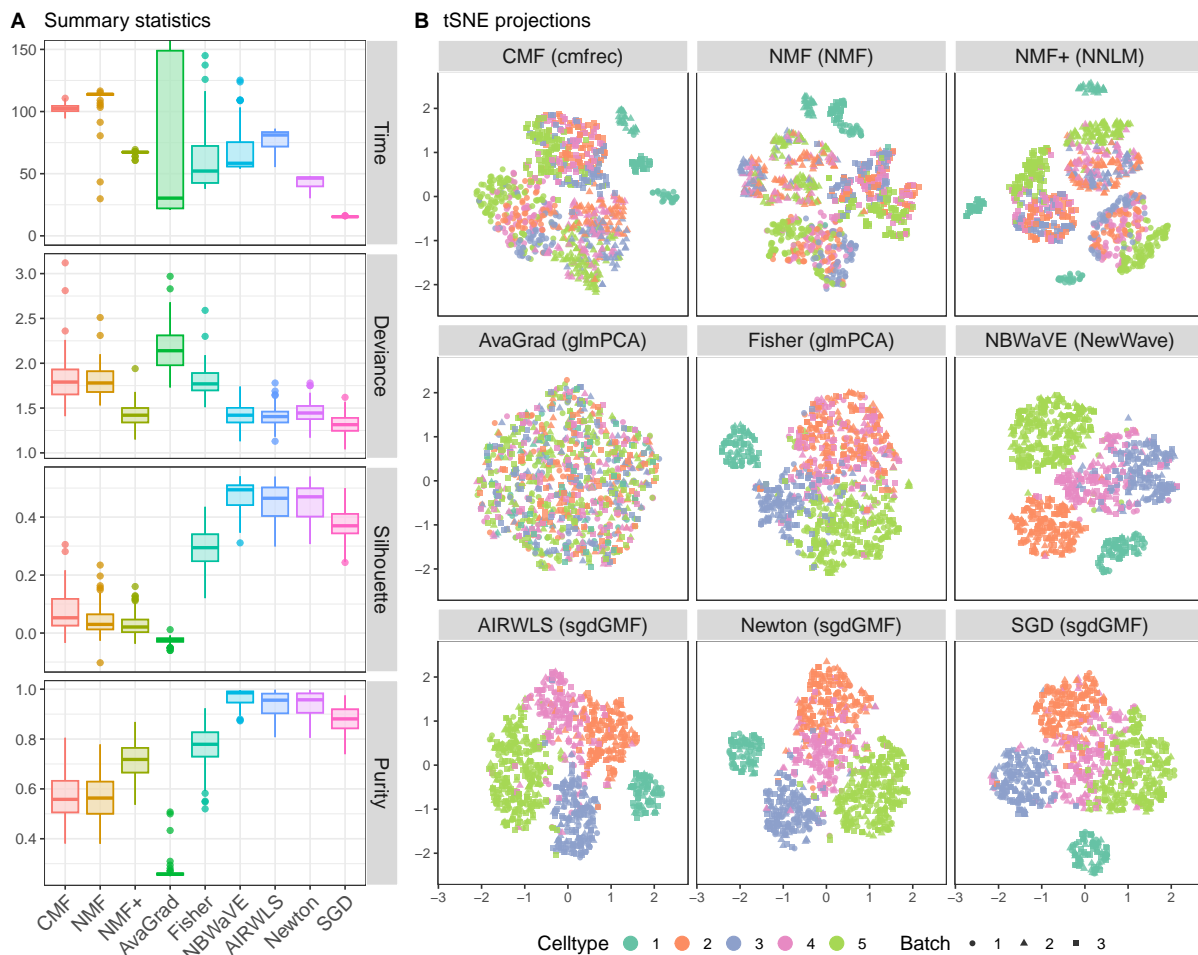


Figure 2: Summary information for the simulation experiment described in Section 5.1 with $n = 5000$, $m = 500$ and $d = 5$. Left: summary statistics reporting the execution time (in seconds), the out-of-sample relative Poisson deviance (multiplied by 100%), the silhouette score of the true cell-type clusters calculated on a 2-dimensional tSNE projection, and the mean cluster purity of the true cell-type clusters calculated on the 5-dimensional estimated latent space. Right: 2-dimensional tSNE projections of the estimated latent factors for one specific replication of the experiment.

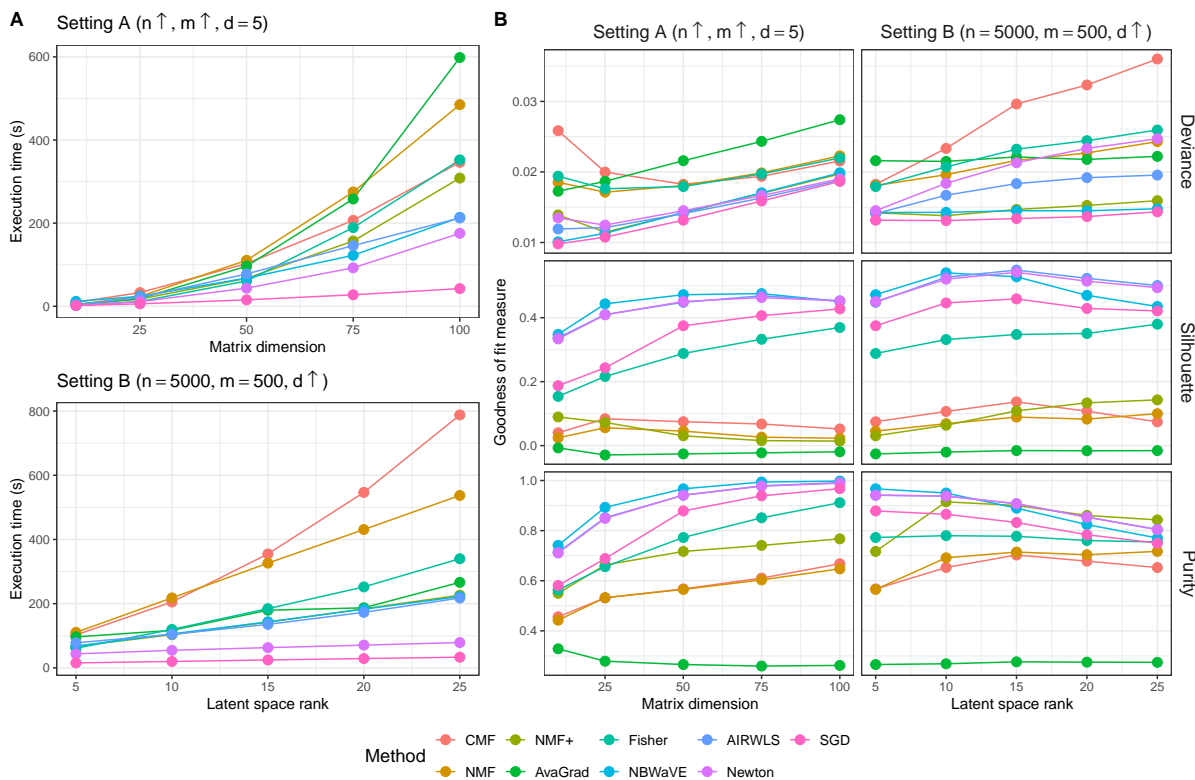


Figure 3: Summary statistics of the simulation experiments described in Section 5.1. Left: elapsed execution time (in seconds) under the simulation settings A and B. Right: goodness of fit measures under the simulation settings A (left column) and B (right column). The considered goodness of fit measures are: the out-of-sample normalized residual deviance, the silhouette evaluated on a 2-dimensional tSNE protection of the latent space, the neighborhood purity of the true cell-type evaluated on the original latent space.

lines with unique driver mutations (Arigoni et al., 2024). As suggested by the authors, the heterogeneity among cell lines can be used as ground truth to benchmark computational methods. We use these data to illustrate that our method can discover real biological signal.

Further, we apply our method to a large scRNA-seq dataset consisting of more than 1.3 million cells from the mouse brain, generated by 10X Genomics (Lun and Morgan, 2023). This dataset showcases the scalability of our approach in large datasets.

Throughout this section, we consider parametrization (B) to obtain an orthonormal loading matrix \mathbf{V} and a scaled orthogonal score factor matrix \mathbf{U} . This choice is conventional in the RNA-seq literature and is coherent with the standard parametrization of principal component analysis.

6.1 Arigoni data

The original Arigoni dataset (Arigoni et al., 2024) consist of 29,606 cells from 8 different cell lines. Quality control is done using the `perCellQCFilters` function of the R package `scuttle` (McCarthy et al., 2017), which filtered cells that have a library size lower than 1306, a percentage of mitochondrial reads higher than 6.05% or cells that have fewer than 732 features expressed. Additionally, peripheral blood mononuclear cells are removed due to their distinct expression profile. The final filtered dataset includes 26,472 cells from 7 different cell lines. Unless mentioned differently, all the analyses are based on the 500 most variable genes, a common choice in standard scRNA-seq workflows.

To select the optimal matrix rank for the latent component of the model, different model selection criteria are assessed in a 5-fold cross validation, assigning missing values to the test partition of each fold. The model selection criteria are shown in Panel A of Figure 4, with Panel B and C showing the evaluation of the model selection criteria. AIC and BIC are assessed on the 5 training data partitions, while the out-of-sample deviance is calculated on the test data. Also, considering all the data, we assess the scree plot of the eigenvalues based on the deviance residuals after using OLS on the log-transformed data.

Both the AIC and out-of-sample deviance criteria suggest a matrix rank of 15, while the BIC and the scree plot suggest 9 (Fig. 4A). The mean cell-line neighborhood purity scores (Fig. 4B) show that, for the majority of cell lines, a rank of 9 is sufficient to completely separate the groups, with only cell lines A549 and CCL-185-IG exhibiting a score lower than 0.9. At rank 15, all cell lines achieve a large value of mean purity and increasing the rank further does not improve this index, while introducing the risk of overfitting the data, as observed in the increasing out-of-sample deviance in the cross validation (Fig. 4A). These remarks are confirmed when visually inspecting the tSNE plots, coloured by the ground truth labels (Fig. 4C), that show that a matrix rank of 9 yields a good separation, except for A549 from CCL-185-IG, which show a slight degree of mixing (Fig. 4C, confusion matrix). Although there are no outstanding visual differences between rank 15 and 30, performing Leiden clustering with a resolution tuned to obtain 7 clusters shows that a matrix of rank 30 results in one small cluster with very few cells, rather than separating the A549 and CCL-185-IG groups, while this happens as expected for rank 15. This suggests that 15 is a reasonable number of latent factors to include in the model.

Using 15 factors, as suggested by the model selection criteria, SGD was compared with NBWaVE, Fisher and AvaGrad, three of the most popular methods in single-cell analysis that perform well in the simulations (Supplementary Fig. 1). All three methods achieve similar results, as shown by both visual inspection of the tSNE plots and the mean cell-line neighborhood purities. However, SGD is orders of magnitude faster, and therefore allows for model selection obtaining optimal matrix rank, which was shown to be important for clustering the data. Further, SGD has a better out-of-sample deviance, probably because it can deal with missing values, unlike NBWaVE and Fisher and AvaGrad which require

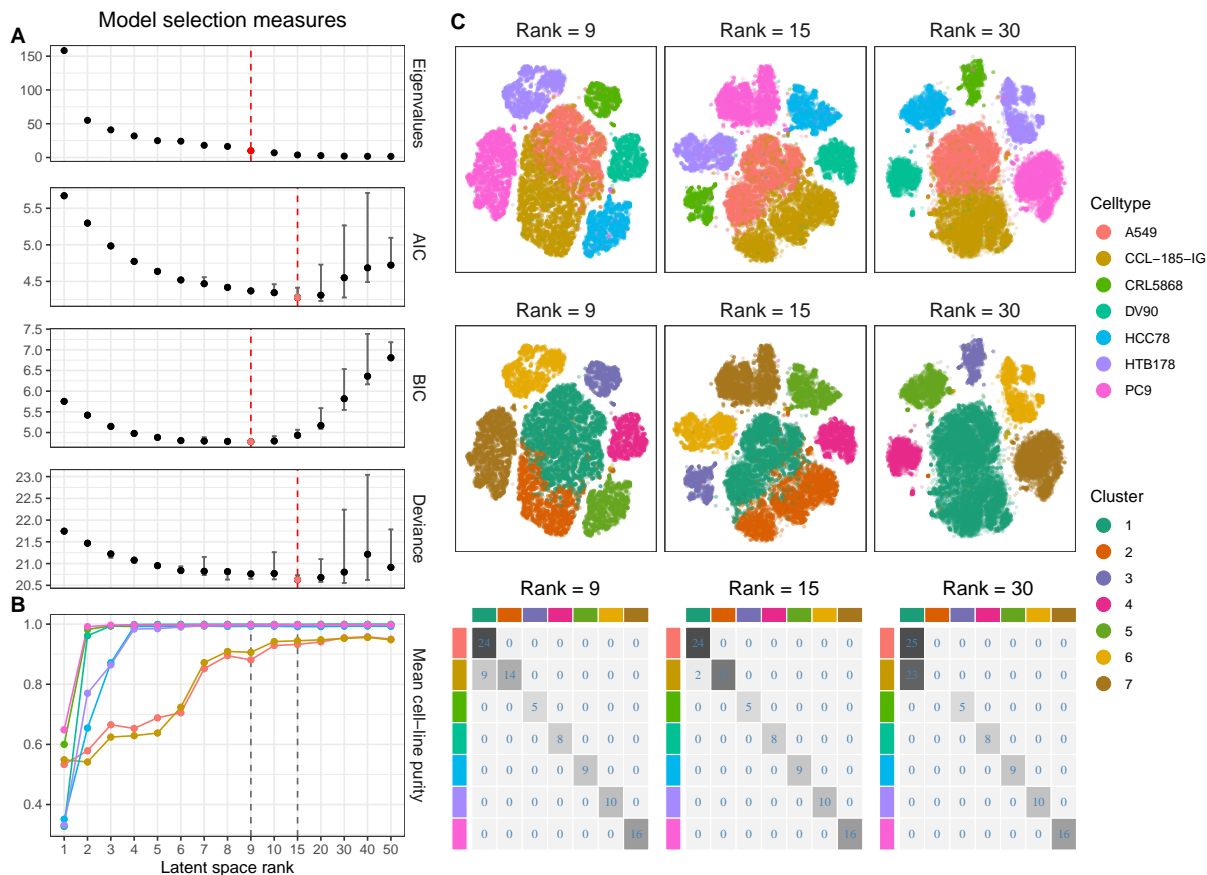


Figure 4: Assessment of model selection metrics. A) Application of diverse model selection criteria including scree plot, AIC, BIC, and cross-validation based on out-of-sample deviances. B) Mean cell-line purity as a function of the matrix rank. C) tSNE plots coloured by the ground truth and clusters obtained by Leiden clustering, alongside a confusion matrix representing cell-line distributions across clusters. In the confusion matrices, each entry is featured with a number corresponding to the percentage of cells belonging to that configuration. The matrix total is equal to 100 and the colour intensity is proportional to the percentages.

imputation.

6.2 TENxBrainData

To demonstrate the scalability of our method to large datasets, we apply SGD to the TENxBrainData (Lun and Morgan, 2023), which consists of scRNA-seq read counts from approximately 1.3 million cells from the mouse brain, generated by 10X Genomics. Quality control and filtering are performed using the R package `scater` (McCarthy et al., 2017), excluding cells with an exceptional number of mitochondrial reads (more than 3 median absolute deviances away from the median), and genes with no expression in over 99% of the cells. This procedure yields 1,232,055 cells and we retain the 500 most variable genes, as done with the Arigoni dataset.

Considering the eigenvalue gap method (Supplementary Fig. 2), which is a very fast procedure for model selection, we selected a model with 10 latent factors, which we were able to fit in 77 minutes with SGD. Subsequent Leiden clustering of this matrix factorization revealed sensible clusters that align with established marker genes (Fig. 5A). For example, cluster 8 is characterized by cells expressing Pyramidal neuron cells marker genes, such as *Crym* (Loo et al., 2019), while cluster 4 contains cells expressing interneurons markers, e.g., *Sst* and *Lhx6* (Tasic et al., 2018).

To study the scalability of SGD and its competitors on this real dataset, we considered subsamples of 100,000, 200,000 and 300,000 cells (Fig. 5B). This analysis showed that SGD is orders of magnitude faster than competing methods, with Fisher and NBWaVE taking 3.5 and 10 hours, respectively, to analyze 300,000 cells. While AvaGrad achieves better computational speed than Fisher and NBWaVE, it still takes more for it to analyze 300,000 cells than for SGD to fit the whole 1.2 million cells. Moreover, AvaGrad did not converge one in five times for 100,000 cells, and two in five times for 200,000 cells.

7 Discussion

In the present work, we propose a flexible and scalable tool to perform generalized matrix factorization in massive data problems, with a particular focus on scRNA-seq applications. We propose an innovative adaptive stochastic gradient descent algorithm, whose performances are enhanced via a memory-efficient block-wise subsampling method and a convenient initialization strategy. An R/C++ implementation in the open-source package `sgdGMF` is freely available on GitHub. Overall, the proposed method proved competitive with state-of-the-art approaches available in R, showing higher prediction accuracy, good biological signal-extraction ability, and a significant speed-up of the execution time in simulated and real data examples. Unlike most methods currently employed for scRNA-seq signal extraction, our approach natively deals with missing values, iteratively imputing them with the model’s current best prediction. This feature proved important for out-of-sample error evaluation, model selection, and matrix completion.

An appealing feature of the proposed method is its flexibility, which enables several extensions and generalizations. The proposed framework naturally extends to heterogeneous likelihood specification across rows or columns of the response matrix. This would make it possible to jointly factorize discrete, count and continuous data sharing the same latent factorization structure, but different conditional distributions. From a biological viewpoint, this extension would permit to flexibly model multi-omic data (Argelaguet et al., 2018, 2020) under the unified framework provided by `sgdGMF`.

Another interesting extension of the proposed algorithm is generalized tensor factorization for non-Gaussian data arrays. In this setting, the computational complexity of estimating highly parametrized models can easily grow very fast. Thus, cheap and modifiable estimation algorithms, such as the proposed adaptive stochastic gradient descent, are becoming increasingly important.

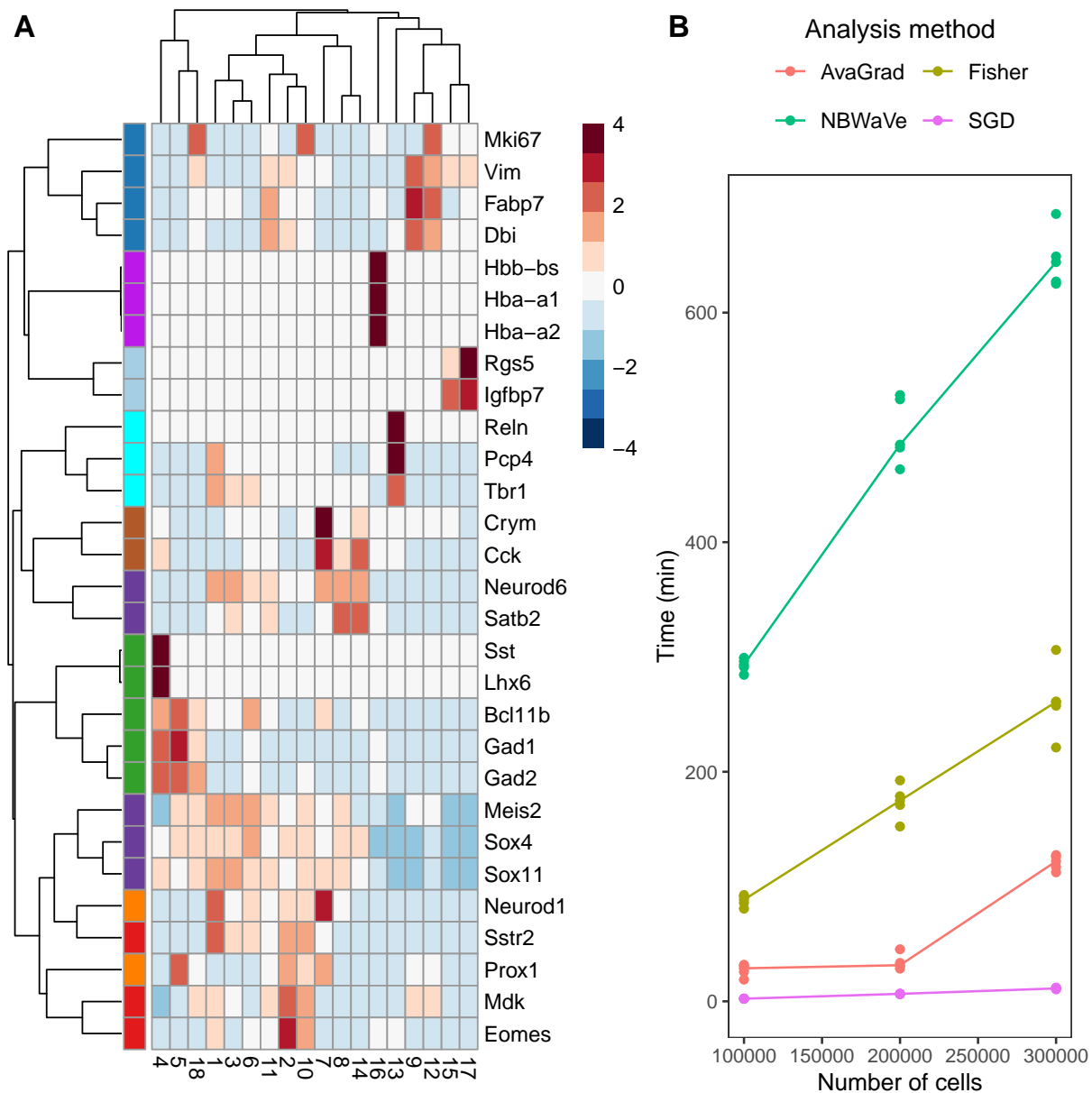


Figure 5: Results on large-scale data. A) Heatmap of the average gene expression of the 18 clusters obtained by Leiden clustering computed on the latent score matrix, for 29 marker genes. Each marker gene is coloured based on the celltype it is expressed in. B) Computational time for different methods on increasingly larger subsets of the dataset. Each subset includes 500 high-variable genes and a growing number of cells.

From an algorithmic viewpoint, another fascinating possibility is considering non-uniform sampling schemes for the mini-batch selection. For instance, if the sample is divided into known subpopulations, it could be convenient to exploit the clustered nature of the data when forming the mini-batch partition via stratification. This can improve the representativeness of each chunk, reduce the variance of the gradient estimator and prevent the optimization from staking on suboptimal maxima dominated by a specific subpopulation signal.

8 Funding

This work was supported by EU funding within the MUR PNRR “National Center for HPC, big data and quantum computing” (Project no. CN00000013 CN1). DR was also supported by the National Cancer Institute of the National Institutes of Health (U24CA289073). The views and opinions expressed are only those of the authors and do not necessarily reflect those of the European Union or the European Commission. Neither the European Union nor the European Commission can be held responsible for them. This work was supported by grants from Ghent University Special Research Fund (BOF20/GOA/023) (A.S., L.C.), Research Foundation Flanders (FWO G062219N) (A.S., L.C.).

9 Data availability

`sgdGMF` is freely available as an open-source R package at [github/CristianCastiglione/sgdGMF](https://github.com/CristianCastiglione/sgdGMF). The scripts used to run all analyses are available on GitHub at [github/alexandresegers/sgdGMF_Paper](https://github.com/alexandresegers/sgdGMF_Paper). The Arigoni dataset is available at <https://doi.org/10.6084/m9.figshare.23939481.v1>. The TENxBrainData dataset is available as part of the `TENxBrainData` Bioconductor package at <https://bioconductor.org/packages/TENxBrainData>.

References

- Agostinis, F., Romualdi, C., Sales, G., and Risso, D. (2022). NewWave: a scalable R/Bioconductor package for the dimensionality reduction and batch effect removal of single-cell RNA-seq data. *Bioinformatics*, 38(9):2648–2650.
- Ahlmann-Eltze, C. and Huber, W. (2023). Comparison of transformations for single-cell RNA-seq data. *Nature Methods*, pages 1–8.
- Angerer, P., Simon, L., Tritschler, S., Wolf, F. A., Fischer, D., and Theis, F. J. (2017). Single cells make big data: New challenges and opportunities in transcriptomics. *Current Opinion in Systems Biology*, 4:85–91.
- Argelaguet, R., Arnol, D., Bredikhin, D., Deloro, Y., Velten, B., Marioni, J. C., and Stegle, O. (2020). MOFA+: a statistical framework for comprehensive integration of multi-modal single-cell data. *Genome biology*, 21(1):1–17.
- Argelaguet, R., Velten, B., Arnol, D., Dietrich, S., Zenz, T., Marioni, J. C., Buettner, F., Huber, W., and Stegle, O. (2018). Multi-Omics Factor Analysis—a framework for unsupervised integration of multi-omics data sets. *Molecular systems biology*, 14(6):e8124.

- Arigoni, M., Ratto, M. L., Riccardo, F., Balmas, E., Calogero, L., Cordero, F., Beccuti, M., Calogero, R. A., and Alessandri, L. (2024). A single cell RNAseq benchmark experiment embedding “controlled” cancer heterogeneity. *Sci. Data*, 11:159.
- Bartholomew, D., Knott, M., and Moustaki, I. (2011). *Latent variable models and factor analysis*. Wiley Series in Probability and Statistics. John Wiley & Sons, Ltd., Chichester, third edition. A unified approach.
- Bianconcini, S. and Cagnone, S. (2012). Estimation of generalized linear latent variable models via fully exponential Laplace approximation. *J. Multivariate Anal.*, 112:183–193.
- Bordes, A., Bottou, L., and Gallinari, P. (2009). SGD-QN: careful quasi-Newton stochastic gradient descent. *J. Mach. Learn. Res.*, 10:1737–1754.
- Bottou, L. (2010). Large-scale machine learning with stochastic gradient descent. In *Proceedings of COMPSTAT’2010: 19th International Conference on Computational Statistics Paris France, August 22-27, 2010 Keynote, Invited and Contributed Papers*, pages 177–186. Springer.
- Breslow, N. E. and Clayton, D. G. (1993). Approximate inference in generalized linear mixed models. *J. Amer. Statist. Assoc.*, 88(421):9–25.
- Cagnone, S. and Monari, P. (2013). Latent variable models for ordinal data by using the adaptive quadrature approximation. *Comput. Statist.*, 28(2):597–619.
- Cai, J.-F., Candès, E. J., and Shen, Z. (2010). A singular value thresholding algorithm for matrix completion. *SIAM J. Optim.*, 20(4):1956–1982.
- Cao, Y., Yang, P., and Yang, J. Y. H. (2021). A benchmark study of simulation methods for single-cell rna sequencing data. *Nature Communications*, 12:6911.
- Cappé, O. and Moulines, E. (2009). On-line expectation–maximization algorithm for latent data models. *J. R. Stat. Soc. Ser. B Stat. Methodol.*, 71:593–613.
- Collins, M., Dasgupta, S., and Schapire, R. E. (2001). A generalization of principal components analysis to the exponential family. *Advances in neural information processing systems*, 14.
- Cortes, D. (2018). Cold-start recommendations in collective matrix factorization. *arXiv preprint arXiv:1809.00366*.
- Cortes, D. (2023). *cmfrec: Collective Matrix Factorization for Recommender systems*. R package version 3.5.1-1.
- Denyer, T., Ma, X., Klesen, S., Scacchi, E., Nieselt, K., and Timmermans, M. C. (2019). Spatiotemporal developmental trajectories in the arabidopsis root revealed using high-throughput single-cell rna sequencing. *Developmental Cell*, 48(6):840–852.e5.
- Duchi, J., Hazan, E., and Singer, Y. (2011). Adaptive subgradient methods for online learning and stochastic optimization. *J. Mach. Learn. Res.*, 12:2121–2159.
- Durif, G., Modolo, L., Mold, J. E., Lambert-Lacroix, S., and Picard, F. (2019). Probabilistic count matrix factorization for single cell expression data analysis. *Bioinformatics*, 35(20):4011–4019.

- Fan, J., Guo, J., and Zheng, S. (2022). Estimating number of factors by adjusted eigenvalues thresholding. *J. Amer. Statist. Assoc.*, 117(538):852–861.
- Friedman, J., Hastie, T., Höfling, H., and Tibshirani, R. (2007). Pathwise coordinate optimization. *Ann. Appl. Stat.*, 1(2):302–332.
- Friedman, J., Hastie, T., and Tibshirani, R. (2010). Regularization paths for generalized linear models via coordinate descent. *J. Stat. Softw.*, 33(1):1.
- Gaujoux, R. and Seoighe, C. (2010). A flexible r package for nonnegative matrix factorization. *BMC Bioinformatics*, 11(1):367.
- Gopalan, P., Hofman, J. M., and Blei, D. M. (2015). Scalable recommendation with hierarchical poisson factorization. In *UAI*, pages 326–335.
- Hicks, S. C., Townes, F. W., Teng, M., and Irizarry, R. A. (2018). Missing data and technical variability in single-cell RNA-sequencing experiments. *Biostatistics*, 19(4):562–578.
- Hinton, G., Srivastava, N., and Swersky, K. (2012). Lecture 6a: Overview of mini-batch gradient descent. https://www.cs.toronto.edu/~tijmen/csc321/slides/lecture_slides_lec6.pdf. Accessed: 2024-02-15.
- Huber, P., Ronchetti, E., and Victoria-Feser, M.-P. (2004). Estimation of generalized linear latent variable models. *J. R. Stat. Soc. Ser. B Stat. Methodol.*, 66(4):893–908.
- Huber, W., Carey, V. J., Gentleman, R., Anders, S., Carlson, M., Carvalho, B. S., Bravo, H. C., Davis, S., Gatto, L., Girke, T., Gottardo, R., Hahne, F., Hansen, K. D., Irizarry, R. A., Lawrence, M., Love, M. I., MacDonald, J., Obenchain, V., Ole’s, A. K., Pag’es, H., Reyes, A., Shannon, P., Smyth, G. K., Tenenbaum, D., Waldron, L., and Morgan, M. (2015). Orchestrating high-throughput genomic analysis with Bioconductor. *Nature Methods*, 12(2):115–121.
- Hui, F. K. C., Warton, D. I., Ormerod, J. T., Haapaniemi, V., and Taskinen, S. (2017). Variational approximations for generalized linear latent variable models. *J. Comput. Graph. Statist.*, 26(1):35–43.
- Jean-Baptiste, K., McFaline-Figueroa, J. L., Alexandre, C. M., Dorrity, M. W., Saunders, L., Bubb, K. L., Trapnell, C., Fields, S., Queitsch, C., and Cuperus, J. T. (2019). Dynamics of Gene Expression in Single Root Cells of *Arabidopsis thaliana*. *The Plant Cell*, 31(5):993–1011.
- Jolliffe, I. (1986). *Principal component analysis: with 26 illustrations*. Springer.
- Kenney, T., Gu, H., and Huang, T. (2021). Poisson PCA: Poisson measurement error corrected PCA, with application to microbiome data. *Biometrics*, 77(4):1369–1384.
- Kharchenko, P. V. (2021). The triumphs and limitations of computational methods for scRNA-seq. *Nature Methods*, 18(7):723–732.
- Kidziński, L. u., Hui, F. K. C., Warton, D. I., and Hastie, T. J. (2022). Generalized matrix factorization: efficient algorithms for fitting generalized linear latent variable models to large data arrays. *J. Mach. Learn. Res.*, 23(291):1–29.
- Kim, S. H. and Cho, S. Y. (2023). Single-cell transcriptomics to understand the cellular heterogeneity in toxicology. *Molecular & Cellular Toxicology*, 19(2):223–228.

- Kingma, D. P. and Ba, J. (2014). Adam: A method for stochastic optimization. *arXiv preprint arXiv:1412.6980*.
- Kiselev, V. Y., Andrews, T. S., and Hemberg, M. (2019). Challenges in unsupervised clustering of single-cell RNA-seq data. *Nature Reviews Genetics*, 20(5):273–282.
- Koren, Y., Bell, R., and Volinsky, C. (2009). Matrix factorization techniques for recommender systems. *Computer*, 42(8):30–37.
- Kouno, T., de Hoon, M., Mar, J. C., Tomaru, Y., Kawano, M., Carninci, P., Suzuki, H., Hayashizaki, Y., and Shin, J. W. (2013). Temporal dynamics and transcriptional control using single-cell gene expression analysis. *Genome Biology*, 14(10):R118.
- Landgraf, A. J. (2015). *Generalized principal component analysis: dimensionality reduction through the projection of natural parameters*. PhD thesis, The Ohio State University.
- Lee, D. D. and Seung, H. S. (1999). Learning the parts of objects by non-negative matrix factorization. *Nature*, 401(6755):788–791.
- Lee, S., Huang, J. Z., and Hu, J. (2010). Sparse logistic principal components analysis for binary data. *The annals of applied statistics*, 4(3):1579.
- Lee, Y., Nelder, J. A., and Pawitan, Y. (2017). *Generalized linear models with random effects*, volume 153 of *Monographs on Statistics and Applied Probability*. CRC Press, Boca Raton, FL, second edition. Unified analysis via H -likelihood.
- Li, J. and Tao, D. (2010). Simple exponential family PCA. In *Proceedings of the Thirteenth International Conference on Artificial Intelligence and Statistics*, pages 453–460. JMLR Workshop and Conference Proceedings.
- Lin, X. and Boutros, P. C. (2020). *NNLM: Fast and Versatile Non-Negative Matrix Factorization*. R package version 0.4.4.
- Liu, W., Lin, H., Zheng, S., and Liu, J. (2023). Generalized factor model for ultra-high dimensional correlated variables with mixed types. *J. Amer. Statist. Assoc.*, 118(542):1385–1401.
- Loo, L., Simon, J. M., Xing, L., McCoy, E. S., Niehaus, J. K., Guo, J., Anton, E., and Zylka, M. J. (2019). Single-cell transcriptomic analysis of mouse neocortical development. *Nature Communications*, 10(1):134.
- Lun, A. and Morgan, M. (2023). `TENxBrainData`: Data from the 10x1.3 million brain cell study. doi:10.18129/B9.bioc.TENxBrainData, R package version 1.22.0, <https://bioconductor.org/packages/TENxBrainData>.
- Mairal, J., Bach, F., Ponce, J., and Sapiro, G. (2010). Online learning for matrix factorization and sparse coding. *J. Mach. Learn. Res.*, 11:19–60.
- Manning, C. D., Raghavan, P., and Schütze, H. (2008). *Introduction to information retrieval*, volume 39. Cambridge University Press.
- Mazumder, R., Hastie, T., and Tibshirani, R. (2010). Spectral regularization algorithms for learning large incomplete matrices. *J. Mach. Learn. Res.*, 11:2287–2322.

- McCarthy, D. J., Campbell, K. R., Lun, A. T. L., and Wills, Q. F. (2017). Scater: pre-processing, quality control, normalization and visualization of single-cell rna-seq data in r. *Bioinformatics*, 33:1179–1186.
- McCullagh, P. and Nelder, J. A. (1989). *Generalized linear models*. Monographs on Statistics and Applied Probability. Chapman & Hall, London, second edition.
- Mensch, A., Mairal, J., Thirion, B., and Varoquaux, G. (2017). Stochastic subsampling for factorizing huge matrices. *IEEE Transactions on Signal Processing*, 66(1):113–128.
- Mohamed, S., Ghahramani, Z., and Heller, K. A. (2008). Bayesian exponential family PCA. *Advances in neural information processing systems*, 21.
- Nesterov, Y. E. (1983). A method of solving a convex programming problem with convergence rate $o(1/k^2)$. In *Doklady Akademii Nauk*, volume 269, pages 543–547. Russian Academy of Sciences.
- Nguyen, T. K. H., Van den Berge, K., Chiogna, M., and Risso, D. (2023). Structure learning for zero-inflated counts with an application to single-cell rna sequencing data. *The Annals of Applied Statistics*, 17(3):2555–2573.
- Niku, J., Warton, D. I., Hui, F. K. C., and Taskinen, S. (2017). Generalized linear latent variable models for multivariate count and biomass data in ecology. *J. Agric. Biol. Environ. Stat.*, 22(4):498–522.
- Onatski, A. (2010). Determining the number of factors from empirical distribution of eigenvalues. *The Review of Economics and Statistics*, 92(4):1004–1016.
- Owen, A. B. and Perry, P. O. (2009). Bi-cross-validation of the SVD and the nonnegative matrix factorization. *Ann. Appl. Stat.*, 3(2):564–594.
- Recht, B. and Ré, C. (2013). Parallel stochastic gradient algorithms for large-scale matrix completion. *Math. Program. Comput.*, 5(2):201–226.
- Reddi, S. J., Kale, S., and Kumar, S. (2019). On the convergence of Adam and beyond. *arXiv preprint arXiv:1904.09237*.
- Risso, D., Perraudeau, F., Gribkova, S., Dudoit, S., and Vert, J.-P. (2018). A general and flexible method for signal extraction from single-cell rna-seq data. *Nature communications*, 9(1):284.
- Robbins, H. and Monro, S. (1951). A stochastic approximation method. *The annals of mathematical statistics*, pages 400–407.
- Rousseeuw, P. J. (1987). Silhouettes: a graphical aid to the interpretation and validation of cluster analysis. *Journal of Computational and Applied Mathematics*, 20:53–65.
- Sammel, M. D., Ryan, L. M., and Legler, J. M. (1997). Latent variable models for mixed discrete and continuous outcomes. *J. R. Stat. Soc. Ser. B Stat. Methodol.*, 59(3):667–678.
- Schein, A. I., Saul, L. K., and Ungar, L. H. (2003). A generalized linear model for principal component analysis of binary data. In *International Workshop on Artificial Intelligence and Statistics*, pages 240–247. PMLR.
- Singh, A. P. and Gordon, G. J. (2008). Relational learning via collective matrix factorization. In *Proceedings of the 14th ACM SIGKDD international conference on Knowledge discovery and data mining*, pages 650–658.

- Smallman, L., Underwood, W., and Artemiou, A. (2020). Simple Poisson PCA: an algorithm for (sparse) feature extraction with simultaneous dimension determination. *Comput. Statist.*, 35(2):559–577.
- Song, Y., Westerhuis, J. A., Aben, N., Michaut, M., Wessels, L. F., and Smilde, A. K. (2019). Principal component analysis of binary genomics data. *Briefings in bioinformatics*, 20(1):317–329.
- Stein-O’Brien, G. L., Arora, R., Culhane, A. C., Favorov, A. V., Garmire, L. X., Greene, C. S., Goff, L. A., Li, Y., Ngom, A., Ochs, M. F., et al. (2018). Enter the matrix: factorization uncovers knowledge from omics. *Trends in Genetics*, 34(10):790–805.
- Street, K., Risso, D., Fletcher, R. B., Das, D., Ngai, J., Yosef, N., Purdom, E., and Dudoit, S. (2018). Slingshot: cell lineage and pseudotime inference for single-cell transcriptomics. *BMC Genomics*, 19:1–16.
- Sun, S., Zhu, J., Ma, Y., and Zhou, X. (2019). Accuracy, robustness and scalability of dimensionality reduction methods for single-cell rna-seq analysis. *Genome biology*, 20(269):1–21.
- Svensson, V. (2020). Droplet scrna-seq is not zero-inflated. *Nature Biotechnology*, 38(2):147–150.
- Tasic, B., Yao, Z., Graybuck, L. T., Smith, K. A., Nguyen, T. N., Bertagnolli, D., Goldy, J., Garren, E., Economo, M. N., Viswanathan, S., et al. (2018). Shared and distinct transcriptomic cell types across neocortical areas. *Nature*, 563(7729):72–78.
- Tipping, M. E. and Bishop, C. M. (1999). Probabilistic principal component analysis. *J. R. Stat. Soc. Ser. B Stat. Methodol.*, 61(3):611–622.
- Toulis, P. and Airolidi, E. M. (2015). Scalable estimation strategies based on stochastic approximations: classical results and new insights. *Stat. Comput.*, 25(4):781–795.
- Townes, F. W., Hicks, S. C., Aryee, M. J., and Irizarry, R. A. (2019). Feature selection and dimension reduction for single-cell RNA-Seq based on a multinomial model. *Genome biology*, 20:1–16.
- Tran, D., Toulis, P., and Airolidi, E. M. (2015). Stochastic gradient descent methods for estimation with large data sets. *arXiv preprint arXiv:1509.06459*.
- Udell, M., Horn, C., Zadeh, R., Boyd, S., et al. (2016). Generalized low-rank models. *Foundations and Trends® in Machine Learning*, 9(1):1–118.
- Van der Maaten, L. and Hinton, G. (2008). Visualizing data using t-sne. *Journal of machine learning research*, 9(11).
- Virta, J. and Artemiou, A. (2023). Poisson PCA for matrix count data. *Pattern Recognition*, 138:109401.
- Wang, L. and Carvalho, L. (2023). Deviance matrix factorization. *Electron. J. Stat.*, 17(2):3762–3810.
- Wang, Y., Bi, X., and Qu, A. (2020). A logistic factorization model for recommender systems with multinomial responses. *J. Comput. Graph. Statist.*, 29(2):396–404.
- Wang, Y.-X. and Zhang, Y.-J. (2012). Nonnegative matrix factorization: A comprehensive review. *IEEE Transactions on knowledge and data engineering*, 25(6):1336–1353.
- Witten, D. M., Tibshirani, R., and Hastie, T. (2009). A penalized matrix decomposition, with applications to sparse principal components and canonical correlation analysis. *Biostatistics*, 10(3):515–534.

- Wu, Y.-F., Chang, N.-W., Chu, L.-A., Liu, H.-Y., Zhou, Y.-X., Pai, Y.-L., Yu, Y.-S., Kuan, C.-H., Wu, Y.-C., Lin, S.-J., and Tan, H.-Y. (2023). Single-Cell Transcriptomics Reveals Cellular Heterogeneity and Complex Cell–Cell Communication Networks in the Mouse Cornea. *Investigative Ophthalmology & Visual Science*, 64(13):5–5.
- Xiang, R., Wang, W., Yang, L., Wang, S., Xu, C., and Chen, X. (2021). A comparison for dimensionality reduction methods of single-cell rna-seq data. *Frontiers in genetics*, 12:646936.
- Yee, T. W. (2015). *Vector generalized linear and additive models*. Springer Series in Statistics. Springer, New York. With an implementation in R.
- Zappia, L., Phipson, B., and Oshlack, A. (2017). Splatter: simulation of single-cell rna sequencing data. *Genome biology*, 18(1):174.
- Zeiler, M. D. (2012). Adadelta: an adaptive learning rate method.
- Zou, H., Hastie, T., and Tibshirani, R. (2006). Sparse principal component analysis. *Journal of computational and graphical statistics*, 15(2):265–286.

Appendices of “Stochastic gradient descent estimation of generalized matrix factorization models with application to single-cell RNA sequencing data”

A Algorithmic details

Unknown dispersion parameter

In the case where the dispersion parameter ϕ is unknown and has to be learned from the data, a standard choice in the literature is the Pearson estimator, which is given by

$$\hat{\phi} = \frac{1}{N} \sum_{i=1}^n \sum_{j=1}^m \frac{(y_{ij} - \hat{\mu}_{ij})^2}{\nu(\hat{\mu}_{ij})/w_{ij}} = \frac{1}{N} \mathbf{1}_n^\top [\mathbf{W} * (\mathbf{Y} - \hat{\boldsymbol{\mu}})^2 / \nu(\hat{\boldsymbol{\mu}})] \mathbf{1}_m.$$

where $N = nm - mp - nq - (n + m)d - 1$ is the effective degrees of freedom of the model, that is the difference between the number of observations and the number of parameters to be estimated. This can be computed *a posteriori* or iteratively refined during the optimization substituting $\hat{\boldsymbol{\mu}}$ with $\boldsymbol{\mu}^t$.

In our optimization routine, we consider a sequential refinement of the dispersion parameter using a smoothed stochastic estimator obtained as

$$\begin{aligned} \hat{\phi}^{t+1} &\leftarrow \frac{1}{N} \frac{nm}{n_i^* m_j^*} \mathbf{1}_{n_i^*}^\top [\mathbf{W}_B * (\mathbf{Y}_B - \boldsymbol{\mu}_B^t)^2 / \nu(\boldsymbol{\mu}_B^t)] \mathbf{1}_{m_j^*}, \\ \bar{\phi}^{t+1} &\leftarrow (1 - \rho_t) \bar{\phi}^t + \rho_t \hat{\phi}^{t+1}, \end{aligned}$$

where $\hat{\phi}^{t+1}$ is the stochastic estimate of ϕ obtained using only the information of the current mini-batch, while $\bar{\phi}^{t+1}$ is a smoothed estimator obtained as the exponential averaging of the current and previous estimates.

Negative Binomial inflation parameter

In the Negative Binomial model, the deviance and variance functions are specified as

$$D_\alpha(y, \mu) = 2w \left[y \log \frac{y}{\mu} - (y + \alpha) \log \frac{y + \alpha}{\mu + \alpha} \right], \quad V_\alpha(\mu) = w\mu(1 + \mu/\alpha).$$

Since the inflation parameter $\alpha > 0$ is typically unknown, we need to estimate it from the data. A common choice in the literature is to consider the moment estimator

$$\hat{\alpha} = \frac{\left[\sum_{i=1}^n \sum_{j=1}^m w_{ij} \hat{\mu}_{ij}^2 \right]}{\left[\sum_{i=1}^n \sum_{j=1}^m w_{ij} \{ (y_{ij} - \hat{\mu}_{ij})^2 - \hat{\mu}_{ij} \} \right]} = \frac{\mathbf{1}_n^\top (\mathbf{W} * \hat{\boldsymbol{\mu}} * \hat{\boldsymbol{\mu}}) \mathbf{1}_m}{\mathbf{1}_n^\top [\mathbf{W} * \{ (\mathbf{Y} - \hat{\boldsymbol{\mu}})^2 - \hat{\boldsymbol{\mu}} \}] \mathbf{1}_m}.$$

where $\hat{\boldsymbol{\mu}}_{ij}$ must be a consistent estimator of the Negative Binomial mean.

Since complete access to the whole data and prediction matrices could be prohibitively expensive in high-dimensional settings, in our optimization scheme, we instead consider the stochastic update

$$\begin{aligned}\hat{\alpha}^{t+1} &\leftarrow \frac{\mathbf{1}_{n_I}^\top (\mathbf{W}_B * \boldsymbol{\mu}_B^t * \boldsymbol{\mu}_B^t) \mathbf{1}_{m_J}}{\mathbf{1}_{n_I}^\top [\mathbf{W}_B * \{(\mathbf{Y}_B - \boldsymbol{\mu}_B^t)^2 - \boldsymbol{\mu}_B^t\}] \mathbf{1}_{m_J}}, \\ \bar{\alpha}^{t+1} &\leftarrow (1 - \rho_t) \bar{\alpha}^t + \rho_t \max(\varepsilon, \hat{\alpha}^{t+1}),\end{aligned}$$

where $\hat{\alpha}^{t+1}$ is the stochastic estimate of α obtained using only the information of the current mini-batch, while $\bar{\alpha}^{t+1}$ is a smoothed estimator obtained as the exponential averaging of the current and previous estimates, and $\varepsilon > 0$ is a small positive constant introduced to ensure that the final estimate is positive.

Initialization details

As explained in Section 3.4 of the main paper, in OLS–SVD initialization, we transform the data according to the perturbed link transformation $y_{\varepsilon, ij} = g_\varepsilon(y_{ij})$, which depends on the control parameter $\varepsilon > 0$, which is typically a small constant. In particular, we consider the following transformation

$$g_\varepsilon(y) = \begin{cases} g(\varepsilon) \mathbb{I}_{\{y=0\}} + g(1 - \varepsilon) \mathbb{I}_{\{y=1\}} & \text{for binary families,} \\ g(\varepsilon) \mathbb{I}_{\{y=0\}} + g(y) \mathbb{I}_{\{y>0\}} & \text{for count families,} \\ g(y) & \text{otherwise,} \end{cases}$$

where \mathbb{I}_A is the indicator function of set A , being equal to 1 when A is satisfied and 0 otherwise.

B Simulation setting details

Data generating process

To simulate the data, we use the R package `splatter` (Zappia et al., 2017), which is freely available on Bioconductor (Huber et al., 2015). In particular, we use the function `splatSimulateGroups()` to generate the gene-expression matrices.

In our experiments, we considered the following simulation setup: each dataset contains cells from five well-separated types evenly distributed in the sample. The data are also divided into three batches having different expression levels. No lineage or branching effects are considered. The setting-specific dimensions of the gene-expression matrices, n and m , are reported in the paper. Under each simulation setting, we set the simulation parameters specifying the following options in the `splatter` functions `newSplatParams()` and `setParams()`:

- number of genes: `nGenes = m`;
- number of cells: `nCells = n`;
- number of cells per batch: `batchCells = c([n/3], [n/3], n - 2[n/3])`;
- probability of each cell-group: `group.prob = c(0.1, 0.2, 0.2, 0.2, 0.3)`;
- probability of gene differential expression in a group: `de.prob = c(0.3, 0.1, 0.2, 0.01, 0.1)`;
- probability of gene down-regulation in a group: `de.downProb = c(0.1, 0.4, 0.9, 0.6, 0.5)`;
- location of the differential expression factor: `de.facLoc = c(0.6, 0.1, 0.1, 0.01, 0.2)`;
- Scale of the differential expression factor: `de.facScale = c(0.1, 0.4, 0.2, 0.5, 0.4)`.

Competing methods

We compare the proposed adaptive stochastic gradient descent method for the estimation of generalized matrix factorization models with several state-of-the-art approaches in the literature. In particular, we consider the following models and algorithms.

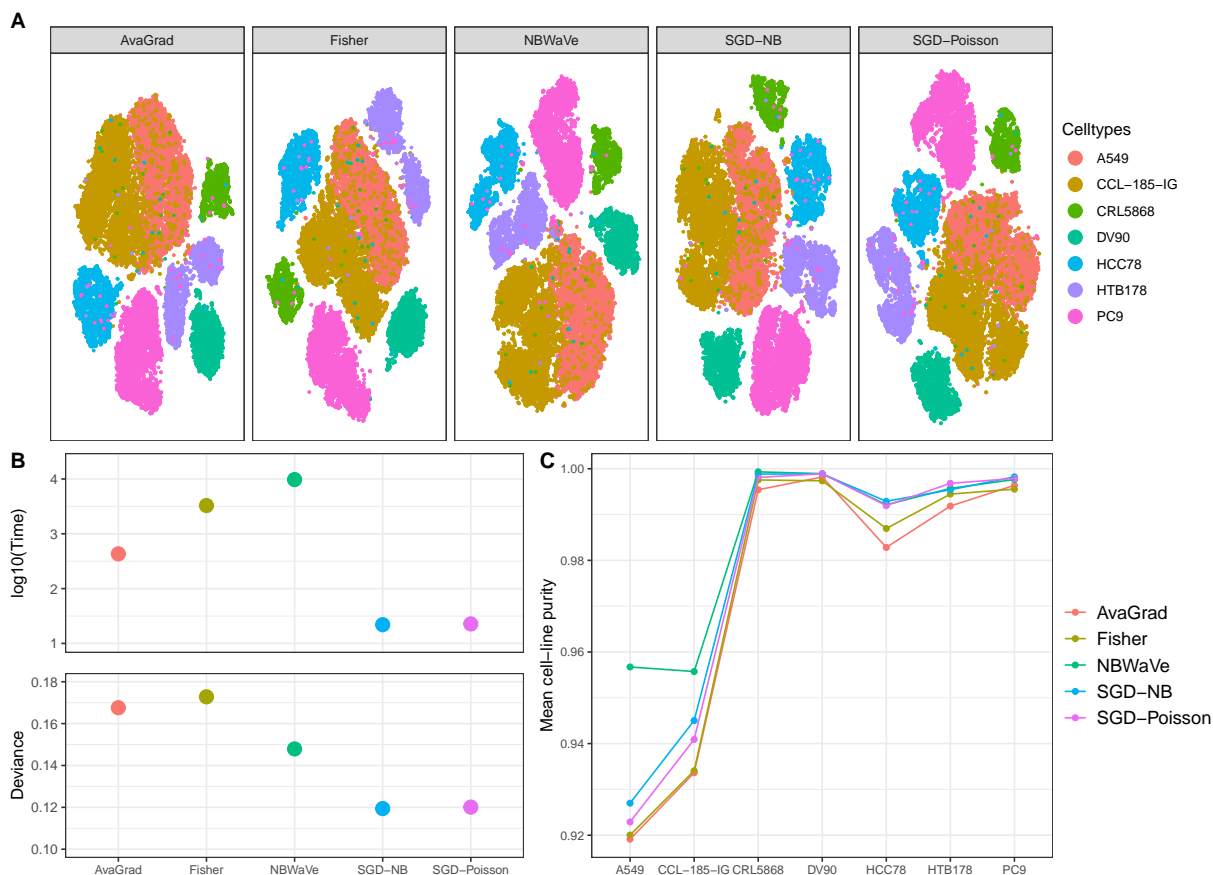
- **CMF**: we use the `CMF()` function in the `cmfrec` package (Cortes, 2023), and we specify the following options: `k = d`, `nonneg = TRUE`, `user_bias = FALSE`, `item_bias = FALSE`, `center = FALSE`, `nthreads = 4`, `niter = 1000`.
- **NMF**: we use the `NMF()` function in the `NMF` package (Gaujoux and Seoighe, 2010), and we specify the following options: `rank = d`, `method = "brunet"`, `seed = "nndsvd"`, `nrun = 1`.
- **NMF+**: we use the `NNMF()` function in the `NNLM` package (Lin and Boutros, 2020), and we specify the following options: `k = d`, `alpha = 1`, `beta = 1`, `n.threads = 4`, `method = "lee"`, `loss = "mkl"`, `max.iter = 2000`.
- **AvaGrad**: we use the `glmpca()` function in the `glmPCA` package (Townes et al., 2019), and we specify the following options: `L = d`, `fam = "poi"`, `minibatch = "none"`, `optimizer = "avagrad"`, `ctl = list(maxIter = 1000, tol = 1e-05)`.
- **Fisher**: we use the `glmpca()` function in the `glmPCA` package (Townes et al., 2019), and we specify the following options: `L = d`, `fam = "poi"`, `minibatch = "none"`, `optimizer = "fisher"`, `ctl = list(maxIter = 200, tol = 1e-05)`.

- **NBWAVE**: we use the `newFit()` function in the `NewWave` package (Agostinis et al., 2022), and we specify the following options: `K = d`, `commondispersion = TRUE`, `maxiter_optimize = 500`, `stop_epsilon = 1e-04`, `children = 4`.
- **AIRWLS**: we use the `cpp.fit.airwls()` function in the `sgdGMF` package, which implement the AIRWLS algorithm of Kidziński et al. (2022) and Wang and Carvalho (2023), and we specify the following options: `ncomp = d`, `familyname = "poisson"`, `linkname = "log"`, `lambda = c(0,0,1,0)`, `maxiter = 200`, `nsteps = 1`, `stepsize = 0.2`, `eps = 1e-08`, `nafill = 1`, `tol = 1e-05`, `damping = 0.001`, `parallel = TRUE`, `nthreads = 4`.
- **Newton**: we use the `cpp.fit.newton()` function in the `sgdGMF` package, which implements the quasi-Newton algorithm of Kidziński et al. (2022), and we specify the following options: `ncomp = d`, `familyname = "poisson"`, `linkname = "log"`, `lambda = c(0,0,1,0)`, `maxiter = 200`, `stepsize = 0.2`, `eps = 1e-08`, `nafill = 1`, `tol = 1e-05`, `damping = 0.001`, `parallel = TRUE`, `nthreads = 4`.
- **SGD**: we use the `cpp.fit.bsgd()` function in the `sgdGMF` package, and we specify the following options: `ncomp = d`, `familyname = "poisson"`, `linkname = "log"`, `lambda = c(0,0,1,0)`, `maxiter = 500`, `rate0 = 0.01`, `size1 = 100`, `size2 = 20`, `eps = 1e-08`, `nafill = 1`, `tol = 1e-05`, `damping = 1e-03`.

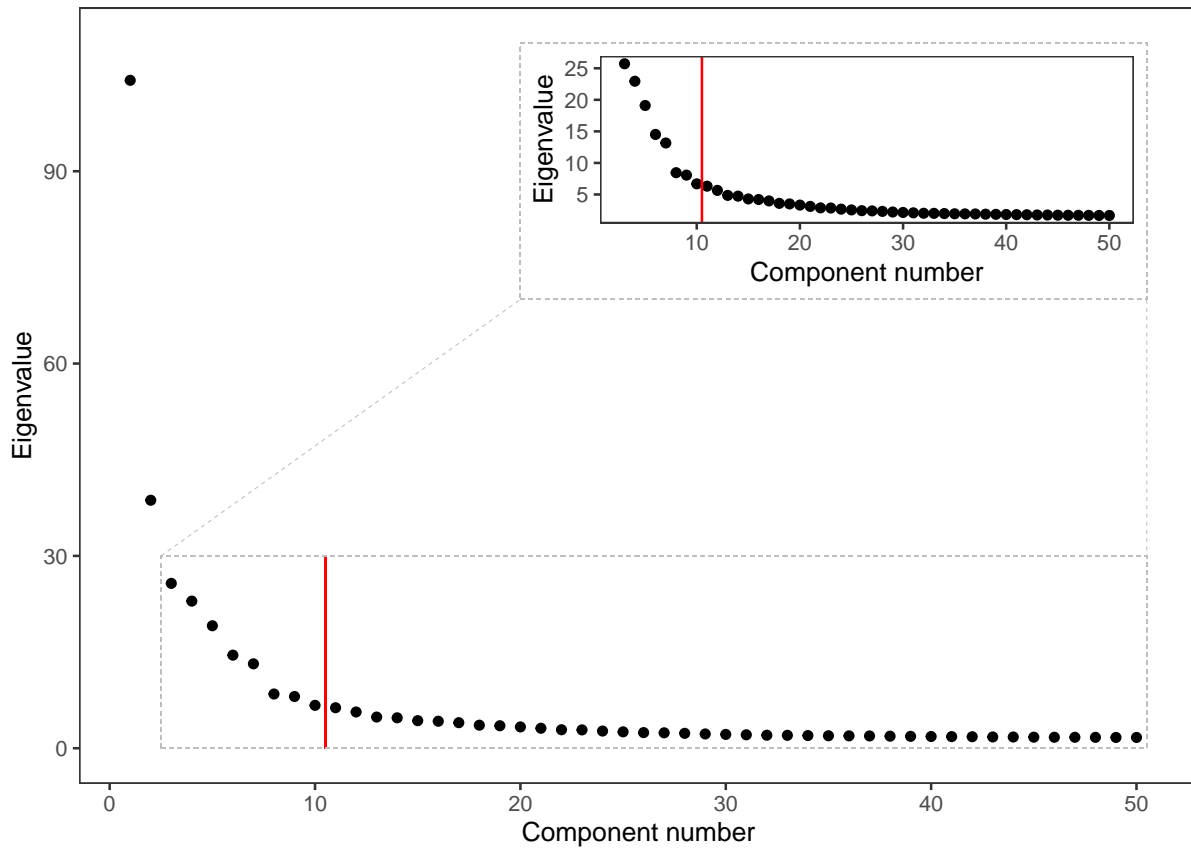
It is worth mentioning that the original R implementation of the AIRWLS and Newton methods can be found in the `gmf` package by Kidziński et al. (2022). However, such an implementation does not permit the inclusion of gene-specific intercepts and covariate effects, say $\gamma_i^\top \mathbf{z}_j$ in our notation, and, also, it does not allow for parallel computing in Windows operating systems. Therefore, we performed the benchmarking experiments using the R/C++ implementation in the proposed `sgdGMF` package.

All the options not specified here are left to default values. For all the R scripts we used for running the simulation and plotting the results, please refer to the GitHub repository `github/alexandresegers/sgdGMF_Paper`.

C Supplementary figures



Supplementary Fig. 6: Comparison of SGD using block-subsampling with NBWaVE (Agostinis et al., 2022) and `glmPCA` (Townes et al., 2019) on the Arigoni dataset (Arigoni et al., 2024). All methods use a matrix rank of 15, which was suggested by model selection criteria. A) tSNE embeddings show no clear differences between all methods. B) SGD is orders of magnitude faster compared to the other methods, and has a lower out-of-sample deviance prediction error when predicting missing values. This is probably due to NBWaVE and `glmPCA` requiring imputation of missing values prior to computation of the latent structure, while SGD can deal with missing values internally. C) The mean cell-line cluster purity is also similar for all methods. SGD gives similar results on all levels when using the Poisson and negative binomial family on the Arigoni dataset. Therefore, SGD is a fast alternative to NBWaVE and `glmPCA`, while having similar performance.



Supplementary Fig. 7: Eigenvalues of the latent directions ordered in descending values for the TEnxBrainData (Lun and Morgan, 2023). This plot, also called an elbow-plot can be used for model selection, by looking for an elbow in the curve. Here, 10 latent factors were chosen to be used in the case study.